NAVAL SHIP RESEARCH AND DEVELOPMENT CENTER

Bethesda, Maryland 20034

PREDICTION OF MOTION AND HYDRODYNAMIC LOADS OF CATAMARANS

by

C.M. Lee, H.D. Jones

and

R.M. Curphey

To be presented at the SNAME Chesapeake Section Meeting on March 14, 1973 at NSRDC

The Naval Ship Research and Development Center is a U. S. Navy center for laboratory effort directed at achieving improved sea and air vehicles. It was formed in March 1967 by merging the David Taylor Model Basin at Carderock, Maryland with the Marine Engineering Laboratory at Annapolis, Maryland.

Naval Ship Research and Development Center
Bethesda, Md. 20034

MAJOR NSRDC ORGANIZATIONAL COMPONENTS

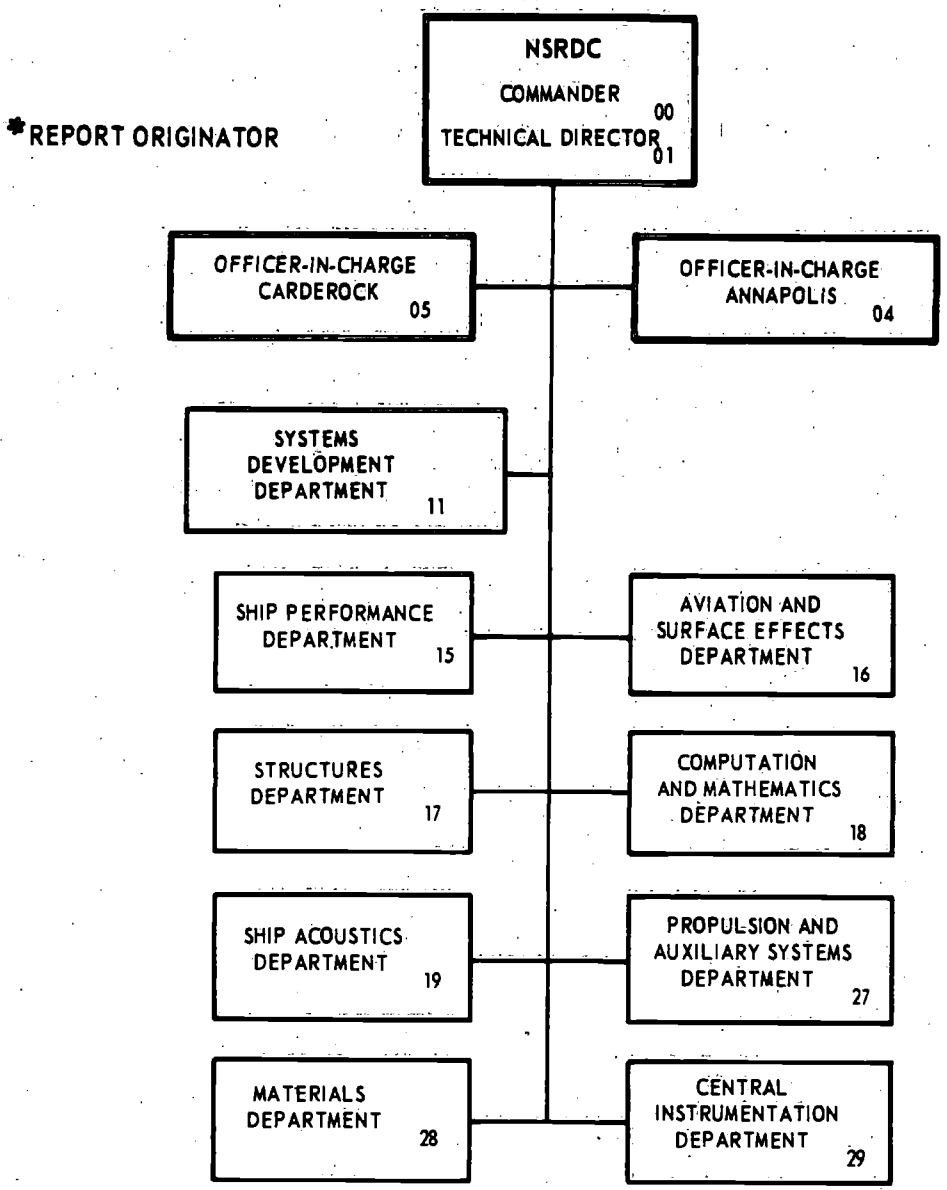

NDW-NSRDC 3960/46 (REV. 8-71)
GPO 917-868

TABLE OF CONTENTS

LIST OF FIGURES

LIST OF TABLES

ABSTRACT

The analytical prediction of catamaran motions in head seas and hydroydnamic loads in beam seas is described. Correlation between the predicted and the model experimental results is presented and discussed.

The analytical prediction is found satisfactory except for some discrepancies resulting from the inadequate account for viscous effects and the three-dimensional hydrodynamic effects.

I. INTRODUCTION

A large useful deck area is one of the obvious advantages associated with catamarans. If this large deck area is to be effectively utilized, it must behave as a stable platform. Thus, the advantages associated with catamaran hull forms may not be fully realized unless they have good seaworthiness characteristics which can compensate for the increased frictional resistance due to the increased wetted hull surface and the added structural problems resulting from the cross-deck structure between the two hulls.

It is a formidable challenge for naval architects to design unconventional hull forms when so little designing data is available. The challenge becomes even more formidable when they have to produce a hull form which not only maintains the expected advantages but also minimizes the penalties inherently associated with the new hull form.

Under such circumstances, the first step to be taken would be to conduct proper research to develop necessary data for catamaran designers. As part of the research efforts at NSRDC in the catamaran area, theoretical and experimental investigations in motion and sea loads of catamarans have been made. The results obtained from these investigations will be presented in this paper.

An analytical method of predicting monohull motion in five-degrees-of-freedom and the sea loads on the ship was developed by Salvesen, Tuck and Faltinsen [1].[1] Based upon a similar approach an analytical method of predicting the coupled heave and pitch motions of catamarans in head seas has been developed [2, 3]. An effort is being made to extend this method to predict all degrees of freedom of motion.

Also, an analytical method of predicting the bending moment, and vertical shear force on the cross-deck structure when stationary catamarans are subjected to beam seas has been developed. Since the head and following waves usually induce largest heave and pitch motion which is most critical from the standpoint of cross-deck impact, and the beam waves acting on a stationary catamaran are regarded as most critical from a hydrodynamic load consideration, the analytical prediction methods presently developed for the head and beam seas can be utilized to investigate the worst conditions for motion and hydrodynamic loads on catamarans.

---

[1] The number in the parenthesis indicates the references listed on page 34.

The correlation between the theoretical values with the model results is found to be reasonably good except for some discrepancies which at present are believed to be caused by viscous effect and by three-dimensional hydrodynamic effect induced by forward speed.

A brief description of the features of motions and hydrodynamic loads normally associated with catamarans is given in Section II. Section III describes the theoretical background for developing the prediction method for the coupled heave and pitch motion. Section IV presents a comparison of the results obtained from theory and experiment. Section V presents the development of the hydrodynamic load prediction and a comparison of theoretical loading results with model experimental results.

II. FEATURES ASSOCIATED WITH THE MOTION AND THE HYDROYDNAMIC LOADS OF CATAMARANS

While an increase in the overall beams in catamarans increases roll stability, this results in a decrease of the natural roll period and tends to make catamarans jerkier than monohull ships. Furthermore, the decrease in the natural period tends to bring the natural periods for roll and pitch closer to each other. This could cause simultaneous excitation of large roll and pitch motions and make extremely uncomfortable riding for the crews.

The existence of the cross-deck structure presents the problem of wave impact on the bottom of the cross-deck structure, when the relative motion between the wave and the ship becomes large. From the viewpoint of the riding comfort of the crew, it is desirable to have small motion with respect to the calm water level. However, from the viewpoint of avoiding the

hydrodynamic impact of the cross deck, a good wave-contouring motion would be desirable.

In this respect, the height of the cross-deck bottom from the calm water level becomes one of the important dimensions in a catamaran design. A lower cross-deck height has advantages in terms of certain catamaran functions such as recovery and drilling operations. It also increases the roll stability by shifting the center of gravity downward which increases the roll restoring moment. Since a considerable amount of the bending moment on the cross deck may be contributed by the net horizontal hydrodynamic forces acting on each hull, lowering of the cross deck would result in a decrease in the bending moment due to a decrease in the moment arm.

On the other hand, the risk of subjecting the deck to impact increases by reducing the deck height. The impact of the cross deck can cause not only structural damage but also damage to onboard instrumentations due to the severe structural vibrations set off by the slam impact.

Another important dimension associated with catamarans is the separation distance between the two hulls. This dimension has direct influence on the roll stability and motion. However, according to the experimental results of ASR and CVA catamaran models, within the separation distance between the inner hulls at the waterline of 70 to 140 percent of the beam of one hull, the effect of the separation distance on the heave and pitch motion and on the hydrodynamic loads on the cross deck does not seem to be appreciable.

Although they are not investigated in the present work, the torsion moments on the cross deck contributed by the differential hydrodynamic loads in pitch and yaw modes are also important factors in catamaran designs.

III. FORMULATION OF MOTION AND DECK SLAMMING

The excitation of motion of ship in regular waves is treated somewhat analogous to the forced oscillation of a simple mass-dashpot-spring system. The equation of motion of such a system in one-degree of freedom can be written as

$$M\ddot{\xi} + B\dot{\xi} + C\xi = F_o \cos\omega t \qquad (1)$$

where $\xi(t) = \xi_o \cos(\omega t + \alpha)$ is the displacement of the body with ξ_o and α denoting the amplitude and phase of the motion and a dot indicating the time derivative, M is the mass, B the damping coefficient, C the spring constant, F_o the ampitude of the exciting force, and ω angular frequency of oscillation.

If we assume that a ship is excited by incoming sinusoidal waves with the encountering frequency ω and that the ship is allowed only to move in the heave mode, then the expression given in Equation (1) could be interpreted as follows: $\xi(t)$ represents the heave motion, M the sum of body mass and the so called added mass, B the coefficient proportional to the average rate of energy dissipated for the generation of outgoing waves by the heave motion, C corresponds to the buoyant restoring force in tons per inch of immersion, and F_o is the amplitude of the wave-exciting force in the vertical direction.

When we allow the body to respond to the wave excitation in six-degrees-of-freedom, coupling among different modes of motion takes place. Thus, if we let $\xi_i(t)$ for $i = 1, 2, \ldots 6$ represent the motion of the ship in surge, sway, heave, roll, pitch and sway, respectively, then a general form of the equations of motion in six-degrees-of-freedom can be represented in the form of

$$\sum_{j=1}^{6} (M_{ii} + A_{ij})\ddot{\xi}_j + B_{ij}\dot{\xi}_j + C_{ij}\xi_j = F_i \cos(\omega t + \beta_i) \qquad (2)$$

for $i = 1, 2, \ldots, 6$.

where M_{ii} is the mass or mass moment of inertia, A_{ij} is the added mass or moment of inertia, B_{ij} the wave-making damping, C_{ij} the restoring constants, F_i the wave-exciting force or moment, and β_i the phase angle with respect to the wave motion above the center of mass of the body.

The motions, ξ_i for $i = 1, 2, \ldots, 6$, are referred to a coordinate system, $Oxyz$, which represents the mean position of the catamaran as shown in Figure 1. The Oxy plane coincides with the calm water surface, and when the catamaran is in its mean position, the Oxz plan coincides with the vertical plane of symmetry of the catamaran. The Oz axis is directed upward and passes through the center of mass, the Ox axis is directed toward the bow and the Oy axis is directed toward the port. Thus, ξ_1 is the displacement of the catamaran from its mean position along the x-axis, ξ_2 is the displacement along the y-axis, ξ_5 is the pitch angle about the y-axis and so forth.

The important underlying assumption in the derivation of Equation (2) is the linear response of the ship in amplitude and frequency to the amplitude and frequency of the exciting wave. This means that when the amplitude of the incoming wave is doubled, the amplitude of ship motion is also doubled, and the frequency of the wave and that of the ship motions are identical.

Since most of the ships have port-and-starboard symmetry, within the linear response theory, the vertical-plane motions and the horizontal-plane motions can be assumed to be decoupled. This means that the surge-heave-pitch motion can be decoupled from the sway-roll-yaw motion. For ships having a slender hull form, we can further assume that the surge motion can be decoupled from the heave-pitch motion.

In this paper, we shall consider only the motion in head-seas which is most critical as far as the slamming of the cross-deck bottom is concerned.

The equations of motion for a coupled heave and pitch motion can be written immediately from (2) as

$$(M + A_{33})\ddot{\xi}_3 + B_{33}\dot{\xi}_3 + C_{33}\xi_3 + A_{35}\ddot{\xi}_5 + B_{35}\dot{\xi}_5 + C_{35}\xi_5 = F_3 \cos(\omega t + \beta_3) \tag{3a}$$

$$(I_5 + A_{55})\ddot{\xi}_5 + B_{55}\dot{\xi}_5 + C_{55}\xi_5 + A_{53}\ddot{\xi}_3 + B_{53}\dot{\xi}_3 + C_{53}\xi_3 = F_5 \cos(\omega t + \beta_5) \tag{3b}$$

where I_5 is the mass moment of inertia about the y-axis. The restoring coefficients are given by

$$C_{33} = \rho g A_w$$

$$C_{35} = \rho g A_w X_F$$

$$C_{55} = \rho g (I_w - \nabla \overline{BG})$$

where A_w is the load waterplane area, I_w the area moment of inertia of the waterplane about the y-axis, X_F the x coordinate of the center of floatation, ∇ the displaced volume, and $\overline{BG}$ the vertical distance between the center of mass and the center of buoyancy.

Under the assumption of a linear response relationship, the solutions for the heave and pitch displacements from the mean position of the catamaran can be expressed by

$$\xi_3(t) = \xi_{30} \cos(\omega t + \alpha_3)$$

$$\xi_5(t) = \xi_{50} \cos(\omega t + \alpha_5)$$

The amplitudes of heave and pitch motions, ξ_{30} and ξ_{50}, and the phase angles, α_3 and α_5, are to be found by solving the Equations (3a) and (3b). Each equation can be decomposed with respect to $\cos\omega t$ and $\sin\omega t$ and, thus the four unknowns can be obtained from the four simultaneous equations.

The main difficulty, however, lies in obtaining the hydrodynamic coefficients, A_{ij}, B_{ij} and F_i for i,j = 3 and 5. These hydrodynamic coefficients are obtained by a strip approximation. This means that at any transverse

section of the catamaran, the hydrodynamic effect on that section is obtained as if the longitudinal variation were negligible. After obtaining the hydrodynamic coefficients per unit length at each transverse section along the length of the ship in the above manner, these quantities are integrated to obtain the total hydrodynamic coefficients. In the evaluation of the sectional hydrodynamic coefficients, the transverse hydrodynamic interaction between the two hulls is taken into account.

Once the heave and pitch motions are known for a given speed and wavelength (or wave frequency), we can apply these results to irregular seas by the principle of linear superposition introduced by St. Denis and Pierson [5]. If we let $\bar{\xi}_i$ be the response amplitude operator (RAO) which is defined by

$$\bar{\xi}_i = \frac{\xi_{io}}{A}, \quad i = 3 \text{ and } 5$$

where A is the wave amplitude and if we let $S(\omega_o)$ denote the Pierson-Moskowitz [6] sea-energy spectrum which is given by

$$S(\omega_o) = \frac{C_1}{\omega_o^5} e^{-C_2/\omega_o^4} \tag{4}$$

where ω_o = wave frequency

C_1 = 0.0081 g; g = gravitational acceleration

C_2 = 33.56/ (significant wave height in feet).

The dimension of $S(\omega_o)$ is $[L^2 T]$ and the scaling unit is governed by that used for the gravitational acceleration, g.

Then, the statistical averages of the amplitude of the motion and of the amplitude of the velocity of the ship can be given, respectively, by

$$\xi_{in} = C_n \left[\int_0^\infty \bar{\xi}_i^2(\omega_o) S(\omega_o) d\omega_o \right]^{1/2} \tag{5a}$$

$$\dot{\xi}_{in} = C_n \left[\int_0^\infty \bar{\xi}_i^2(\omega_o) \omega^2 S(\omega_o) d\omega_o \right]^{1/2} \tag{5b}$$

where $i = 3$ or 5

$n = 1/2, 1/3$, or $1/10$

$C_{1/2} = 1.253$: mean average

$C_{1/3} = 2.0$: 1/3 highest average

$C_{1/10} = 2.546$: 1/10 highest average

Hydrodynamic Impact of Cross-Deck Bottom

In the case of bow slamming of monohull ships, not only the relative bow displacement but also the relative velocity with respect to the free surface should exceed certain limits to induce slamming. The limit for the relative velocity to cause slamming is often called the threshold velocity. The phenomenon which causes hydrodynamic impact on the catamaran cross-deck is somewhat different from the slamming of a ship bow. Ochi and Bonilla-Norat [7] have shown that the impact pressure resulting from the reentry of a ship fore body into waves is significantly different from that resulting from dropping of the fore body into the water surface.

The cross-deck impact would be more closely related to the latter case. For the case of the catamaran cross-deck, the presence of two side walls would seal off the escape of water when contact with the free surface is made. Thus, the cross-deck bottom may be more vulnerable to a hydrodynamic impact than the bottom of ship bow when free surface contact is made.

In order to predict the hydrodynamic impact of the bottom of the catamaran cross deck, we need to know the relative vertical displacement between the cross deck and the free surface beneath the deck. The worst condition for a deck impact would arise when the vertical motions of the cross deck and the free surface are 180 degrees out of phase, and the amplitudes of their motions are large.

The vertical displacement of a point on the cross-deck bottom at the distance x from the longitudinal center of gravity is the sum of the heave displacement and the product of the pitch angle and the moment arm x. That is, if we denote the maximum vertical displacement of that point by Z_o which is caused by a train of regular head waves, we have

$$Z_o(x) = \xi_3(t) - x\xi_5(t)$$

where the minus sign is due to our definition of pitch being positive when the bow is down. Then the vertical displacement, Z_R, of the point from the wave surface can be obtained by

$$Z_R(x) = Z_o(x) - \zeta(x)$$

where $\zeta(x)$ denotes the wave elevation from the calm water level. If the absolute magnitude of $Z_R(x)$ exceeds the clearance, C_o, between the calm water level and the cross-deck bottom, i.e., $|Z_R| > C_o$, water contact with the deck bottom can be expected.

The worst sea condition to induce sever cross deck impacts would be periodic waves such as a swelled sea having a period close to the natural period of the ship. Thus, the above analysis for regular waves would yield an overprediction of occurrence of deck impact for most irregular sea conditions. The analysis, however, can be easily extended to irregular seas if we assume a truncated Rayleigh's probability distribution for deck impact as normally done in the case of monohull ships [8]. The number of impact of the cross deck located at x distance from the center of gravity during N hours in a seaway can be obtained by

$$N_s = \frac{1800N}{\pi}\sqrt{\frac{E_v}{E_d}}\exp\left(-\frac{C_o^2}{2E_d}\right) \tag{6}$$

where

$$E_d = \int_o^\infty [\bar{Z}_{RO}(\omega_o; x)]^2 S(\omega_o)d\omega_o \quad = \text{Variance of relative vertical displacement}$$

$$E_v = \int_o^\infty [\omega\, \bar{Z}_{RO}(\omega_o; x)]^2 S(\omega_o)d\omega_o \quad = \text{Variance of relative vertical velocity}$$

In the above Equations $S(\omega_o)$ is the Pierson-Moskowitz spectrum as given in Equation (4), $\bar{Z}_{RO}$ the ratio of the relative vertical displacement of the deck to the wave amplitude, and C_o the clearance of the cross-deck bottom from the mean water level.

IV. COMPARISON OF THEORETICAL RESULTS WITH MODEL EXPERIMENTAL RESULTS

The experimental verification was carried out by first conducting experiments with two dimensional twin hulls to determine their heave added mass and damping coefficients. This verification is important since the strip evaluation of the hydrodynamic coefficients is based on a two-dimensional flow assumption for each cross section. The two-dimensional experiment was then followed by experiments with an early ASR catamaran design to determine its coefficients in the coupled heave and pitch equations of motion. The verification was then followed by making a comparison of the predicted regular-wave motions with experimentally obtained results for various catamaran hull forms.

Two-Dimensional Experiments

Cylindrical-type models, each consisting of two wooden hulls 7.5 feet in length, were tested to determine their heave added mass and damping coefficients [9]. The twin-hull configurations that were tested consisted of semicircles, rectangles, isosceles triangles and right triangles.

In order to approach the desired two-dimensional case, a piece of one-half inch plywood (3 X 7.5 ft) was attached vertically at each end of the twin-hull configurations. This also served as rigid coupling between the hulls. To minimize oscillation of these end boards and to improve rigidity, the boards were reinforced with aluminum angles on the outside as shown in Figure 2. Also shown in this figure is the complete model setup with the X-frame used to attach the model to the oscillation. The models were then oscillated vertically and the forces encountered were measured. These forces were then analyzed to determine the added mass

and damping coefficients. This was done over a range of frequencies with linearity checks for the amplitude of oscillation carried out in the midfrequency range.

Two-Dimensional Results

Results will only be presented here for two of the cases investigated. However, they were selected to represent the extremes in correlation. The figures are presented with the experimentally determined results compared to the theoretically predicted values. Figure 3 shows the added mass and damping coefficients for the twin semicircular cylinders for $b/a = 1.5$ where b is the separation distance between the centerplane of the two hulls and that of one hull, and a is the half beam of one hull. The agreement seen here between theory and experiment is good, however, the damping does show some disagreement in the low frequency range. Figure 4 gives the added mass and damping coefficients for the twin right triangles for $b/a = 4$. Here larger discrepancies can be seen in the agreement between the experimental and theoretical results in the low frequency range; however, the agreement still remains good over the remainder of the frequency range tested.

Three-Dimensional Experiments

The results of several catamaran model experiments were used in the validation of the computed predictions. The most extensive work was carried out using a model of an early design of the ASR catamaran mothership intended to service the Deep Sea Rescue Vehicle. Data from other catamaran experiments were also used; however, only those from the large CVA MODCAT which is of

SWATH configuration will be presented here to show the range of correlation that was found. The main characteristics of these designs are given in Table 1 and the body plans are given in Figure 5.

The experiments using the ASR model were conducted as (1) forced oscillation tests to obtain the added mass and damping coefficients. (2) restrained model tests to obtain the wave-exciting force and moment and (3) model motion tests in waves to obtain the heave and pitch motions.

The forced-oscillation experiments were conducted with a 12.4 foot model (designated 5061) of the early ASR design. This model consisted of two rigid wooden hulls with asymmetric forebodies and symmetric afterbodies rigidly coupled by four wooden cross beams.

The model was first forced to heave sinusoidally at the free surface of the water in the same manner as described for the two-dimensional models. The model was then forced to pitch sinusoidally. This was accomplished by restraining the model at the LCG, so that it was free to pivot about a point coincident with the LCG and the design waterline, and forcing it sinusoidally at the stern. These experiments were carried out over a range of frequencies and at various forward speeds with linearity checks with several amplitudes of oscillation performed over the mid-frequency range.

The regular wave exciting forces and moments were determined by restraining the model at the free surface and measuring the forces imposed as the waves passed. These tests were conducted at various forward speeds in regular head waves ranging in wavelength to ship length ratio from 0.9 to 2.0 with a predominant wave steepness ratio (wave height/wave length) of about 1/50.

The motion data for the ASR were obtained by attaching the self-propelled model, floating at its design waterline, to the carriage by means of the Center's motion measuring apparatus. This apparatus allows the model to respond in all six modes and measures these responses by means of linear potentiometers. These self-propelled model experiments were carried out at Froude numbers of 0, 0.104, 0.311, and 0.414, in wavelength to ship length ratios of 0.5 to 3.5 in the Center's Maneuvering and Seakeeping Basin.

The MODCAT motion data were obtained using a 17.0 foot model (5266) designed to represent a large CVA MODCAT catamaran [10]. These experiments were carried out with the model self-propelled and free to move in all six modes. The only couplings between the model and the carriage were the cables to the electronic measurement devices and those needed for model power and control, together with the flexible tethering lines required to accelerate and decelerate the model. During the time data were taken, all connections were slack and did not affect the model motions. These experiments were carried out at Froude numbers of 0, 0.153, and 0.306 in wavelength to ship length ratios of 0.40 to 4.90 in the same facility as the ASR.

Three-Dimensional Results

For the ASR, the comparisons of the coefficients in the coupled heave and pitch equations of motion are given in Figures 6 through 8. Here the results for one Froude number, i.e., $F_n = 0.126$, were selected, however, they are fairly representative of the overall results. The results are plotted against the nondimensional frequency, $\omega\ L/g$. In general, there is fair to good agreement with some exceptions usually at higher Froude

numbers. Figure 6 shows the heave added mass and damping. Here the agreement is good with the exception of the lower predicted minimum seen in the damping. In Figure 7 it may be seen that for the pitch added moment of inertia and damping, the results compare similar to the heave coefficient. However, in the region of the minimum in the added moment of inertia there appears to be more nonlinearity with oscillation amplitude than is seen in the heave coefficients. Table 2 compares the experimentally determined values for the restoring coefficients with those predicted analytically. Here again better agreement is seen in the heave coefficient than in pitch. The cross coupling terms show generally similar trends as seen above. The heave exciting force and pitch exciting moment parameters are shown in Figure 8. The comparison seen here in the heave exciting force is quite good, however, the analytically predicted pitch exciting moment grossly overpredicts the values determined experimentally. The phases for the forces and moments are not inserted here; however, the agreement is quite good.

The validation of the motion predictions is given in Figures 9 and 10. The heave and pitch results for the ASR are given in Figure 9 for a Froude number of 0.104. The agreement between the experimentally determined values and those predicted analytically is good for this speed. It is seen in other results for higher Froude numbers that the analytical procedure begins to overpredict peak values. The results for the large CVA MODCAT are presented in Figure 10 for a Froude number of 0.153. Here the analytically predicted values compare well over most of the range except for a grossly overpredicted resonance. The zero-speed results showed good agreement while the higher speed showed an overpredicted resonance.

The discrepancies observed in the comparison of the theoretical values with the experimental results are understood to stem largely from the shortcomings of the theory in the evaluation of the damping coefficients. Two factors contributing to this might be the neglect of the viscous effects and of the three-dimensional hydrodynamic effects.

When the damping mechanism of ship motion is mainly contributed by the wave-making effect, the viscous damping may not have noticeable effect on ship motion. However, when the relative magnitude of the viscous damping is no longer negligible compared to the wave-making damping, e.g. a heaving SWATH, the computed ship motion based on the wave-making damping alone would be inaccurate, especially at the vicinity of the resonant frequencies.

The strip approximation of the hydrodynamic coefficients is based on the two-dimensional flow assumption at each cross section. That is, when a catamaran undergoes heave motion in calm water without forward speed, the hydrodynamic force acting upon a cross section of the catamaran is assumed to be unaffected by the presence of the neighboring fore and aft cross sections. One of the possible shortcomings of this assumption in the case of catamarans is an overestimation of hydrodynamic interactions between the two hulls. With the two-dimensional flow assumption at each cross section, the waves generated by motion should propagate outward in the plane of the cross section. Thus, between the space of two hulls, the waves created by each hull would propagate opposite to each other and actively interact. In reality, when the catamaran has a forward speed, the propagation of the waves created by the motion of each hull would not be in the same plane of the cross section but would

be swept backward. This would somehow reduce the hydrodynamic interaction effect which is obtained by the two-dimensional theory.

V. STRUCTURAL LOADING ON CATAMARANS IN BEAM WAVES

The bending moment, vertical shear force, and horizontal shear force acting on the cross-beam structure of a catamaran with zero forward speed in regular and irregular beam waves will be of interest in this analysis.

The mathematical model presented here applies for catamarans of either a conventional hull shape or small-waterplane-area-twin hulls (SWATH). It is assumed that the hulls are symmetric about the vertical center plane and also posses a sufficient degree of longitudinal symmetry such that only sway, heave, and roll modes of motion are excited by the incident beam waves.

With no pitching or yawing motion, the three-dimensional motion and loading problem has been simplified to one of finding the motion and loading of an equivalent two-dimensional body. The equivalent two-dimensional hull form is generated from the midship section of the catamaran in question. The midship section is then taken to be uniform over an equivalent length such that the actual displacement of the ship is obtained.

A midship cross section of a conventional catamaran is shown in Figure 11. A coordinate system Oyz is fixed at the intersection of the centerline of the ship section and the mean water surface and a plane sinusoidal wave with amplitude, A, is progressing in the positive y direction. The beam, B_m, draft, T , and separation distance, b, of

the hulls are shown in Figure 11. The height of the neutral axis of the cross-beam structure above the mean water surface is indicated by h_o. The vector, $\vec{n}$, is the unit surface normal on the submerged portion of the hulls with components n_2 and n_3 in the y and z axes, respectively. Positive sway, ξ_2, and heave, ξ_3, are small displacements of the ship from the equilibrium position in the positive y and z directions, respectively, and a positive roll, ξ_4, is the angular displacement from equilibrium in a counterclockwise direction.

The conventions for bending moment and shearing forces acting on the cross-beam structure are indicated in Figure 12. The bending moment is the moment which tends to roll the hulls relative to each other or equivalently to sag or hog the cross-beam. Positive bending moment is defined as the moment which tends to roll the right hull in a counterclockwise direction or the left hull in a clockwise direction. Positive bending would result from the action of a positive vertical and positive horizontal force acting on the right hull or a positive vertical force and negative horizontal force acting on the left hull (see Figure 12a). Vertical and horizontal shears are respectively the forces which tend to heave and sway the hulls relative to each other. Positive vertical shear is defined as the force which tends to heave the right hull upward or the left hull downward, and would result from the action of a positive vertical force on the right hull or a negative vertical force on the left hull (see Figure 12b). Positive horizontal shear is defined as the force which tends to sway the right hull to the right or the left hull to the left, and would result from the action of a positive horizontal force on the right hull or a negative horizontal force on the left hull. (see Figure 12c).

Theory

As the incident beam wave propagates past the body, a pressure distribution is established over the hulls which tends to excite motion in sway, heave, and roll, and produces structural loading at points on the section. As motion is excited additional forces and loads due to the motion itself are generated, and if we assume that the hydrodynamic pressure distribution, wave exciting forces, motion, and loads are all linear in amplitude and frequency with respect to the incident sinusoidal wave, a linear analysis in the frequency domain can be pursued.

The motion of the catamaran section can be determined by the solution of the equations of motion given below.

$$\text{Heave:} \quad (M'+A'_{33})\ddot{\xi}_3+B'_{33}\dot{\xi}_3+C'_{33}\xi_3 = F'_3 \cos(\omega t+\beta'_3) \tag{7a}$$

$$\text{Sway:} \quad (M'+A'_{22})\ddot{\xi}_2+B'_{22}\dot{\xi}_2+A'_{24}\ddot{\xi}_4+B'_{24}\dot{\xi}_4 = F'_2 \cos(\omega t+\beta'_2) \tag{7b}$$

$$\text{Roll:} \quad (I'_4+A'_{44})\ddot{\xi}_4+B'_{44}\dot{\xi}_4+C'_{44}\xi_4+A'_{42}\ddot{\xi}_2+B'_{42}\dot{\xi}_2 = F_4 \cos(\omega t+\beta'_4) \tag{7c}$$

Where M' is the mass of the section and the definition of the hydrodynamic coefficients A'_{ij}, B'_{ij}, and F'_i and the phase angles β'_i for $i, j = 2,3,4$ are given as in Equation (2) except that the primes denote two-dimensional quantities, I'_4 is the mass moment of inertia in roll, $C'_{33} = 2\rho g x$ (demihull beam), and $C'_{44} = M'g\ \overline{GM}$.

Once the motion is known, the loading may be computed. In general the structural loading may be resolved into the following contributing effects.

1. Incident wave; this component of the structural loads arises from the pressure distribution of the undisturbed incident wave over the body, when the body is restrained from moving and is assumed not to disturb the incident wave. This assumption is commonly called the Froude-Krylov hypothesis.

2. Diffraction; this component accounts for the scattering of the incident wave by the presence of the body. When summed with the incident wave effect, the two contributions provide the structural loading on a body section which is restrained from moving.

3. Motion; as mentioned previously when the body undergoes motion, additional loads due to the motion itself are established. These are a result of the mass-acceleration, buoyant restoring, and hydrodynamic (added mass and wave-making damping) effects.

Structural Loading

In order to find the loading at the midpoint of the cross-beam, a standard approach of structural analysis would be to cut the body section at the point where the loading is to be determined and consider all of the forces and moments (both inertial and hydrodynamic) acting on the free end. If the portion of the section to the right of the cut is taken to be the free end as in Figure 13a, the moment and shears are given by the mass-acceleration effects at the free end minus an integral of the

pressure over the submerged portion of the free end in a sense which provides the moment or force in a given direction.

The loading at $y=0$ and $z=h_o$ is then given by

$$\text{Bending Moment:} \quad M = M_I - \int_R p[n_3 y + n_2(h_o - z)]dl \tag{8}$$

$$\text{Horizontal Shear:} \quad V_2 = V_{2I} - \int_R pn_2 dl \tag{9}$$

$$\text{Vertical Shear:} \quad V_3 = V_{3I} - \int_R pn_3 dl \tag{10}$$

where M_I, V_{2I}, and V_{3I} are mass-acceleration effects of the free end portion and in general depend on all modes of motion, p is the hydrodynamic pressure, and R denotes integration over the submerged portion of the demihull on the right. The same loading quantities must also be obtained if the left hull is taken to the free end and all forces and moments acting on the left hull are considered as in Figure 13b.

The equality at these two approaches suggests a third equivalent method in which the effects from both the right and left hulls are added together with a sign consistent with the loading conventions as shown in Figure 13a and 13b and the resulting quantity divided by two [11]. The advantage of this approach is that the equations for the loading may be

written for the full body section, and when the loads are then evaluated at the midspan of the cross-beam, use may be made of the symmetic and antisymmetric nature of the mass-acceleration effects and pressure distribution with respect to the centerline to greatly simplify the loading analysis.

This can be seen as follows. If the body is restrained from moving, a positive vertical force acting on the right hull tends to produce a positive bending moment and positive vertical shear (see Figure 13a), but the same positive vertical force acting on the left hull produces a positive bending moment and a negative shear (see Figure 13b). The summation of the bending and vertical shear from each hull gives twice the bending moment but no vertical shear. It may then be concluded that a vertical force on the body which is symmetric with respect to the centerline will produce a bending moment but no vertical shear and a vertical force which is antisymmetric with respect to the centerline will produce no bending moment but a vertical shear. It is interesting to note such a symmetric and antisymmetric vertical force arrangement has just the opposite effect on body motion. That is, an even vertical force produces heave but no roll, and an odd vertical force produces roll but no heave.

An analagous argument can be made for the case of horizontal forces acting on each hull. An antisymmetric horizontal force produces both a bending moment and horizontal shear but no roll or sway motion (see Figure 13c). A symmetric horizontal force produces no bending or horizontal shear but does tend to produce roll and sway.

The mass-acceleration components at the midspan also indicate a similar symmetric and antisymmetric nature in their contribution to loading. If the catamaran section it artifically forced to oscillate in sway, heave, and roll in vacuum, only heaving can produce bending, only rolling can produce vertical shear, and no mass acceleration component affects the horizontal shear.

Once the loadings at the midsection of the cross beam are known, then the loading at any section above the waterline can be found. This is done by subtracting the contribution made by the mass inertia of the portion of the structure member between the midsection and the section in question from the already known loadings at the midsection of the cross beam.

Expressions for the structural loading at the mid-beam may now be rewritten in the following form where mass-acceleration and the hydrodynamic pressure components are evaluated over the full body section.

Bending Moment:
$$M = 1/2M'\bar{y}\ddot{\xi}_3 - 1/2 \int_{R+L} p[n_3|y| + n_2(h_o - z)\mathrm{sgn}(y)]dl \quad (11)$$

Horizontal Shear:
$$V_2 = -1/2 \int_{R+L} p[n_2 \mathrm{sgn}(y)]dl \quad (12)$$

Vertical Shear:
$$V_3 = -1/2M'\bar{y}\ddot{\xi}_4 - 1/2 \int_{R+L} pn_3 \mathrm{sgn}(y)dl \quad (13)$$

where M' is the mass of the full body section, $\bar{y}$ is the y coordinate of the center of mass of one hull, $\ddot{\xi}_3$ and $\ddot{\xi}_4$, are respectively the heave and roll accelerations, sgn(y) denotes sign of y, and R+L denotes integration over the submerged portion of the right and left hulls.

It is interesting to note that given any arbitrary pressure distribution, only the symmetric part of pressure with respect to y=0 can contribute to the bending moment and horizontal shear at the midspan, and only the antisymmetric part can contribute to the vertical shear.

In order to evaluate the loading it remains to determine the pressure distribution on the body section and the motion response. The pressure, as mentioned previously, in general has components due to the incident and diffracted waves, and motion, including added mass, damping, and restoring effects. The pressure can be determined from potential flow theory, and the sway, heave, and roll motion obtained by solution of the equations of motion as given in Equation (7).

In summary, the mathematical model predicts that the incident and diffracted wave effects contribute to all load quantities, however, bending moment and horizontal shear are affected only by heaving motion, and the vertical shear is affected only by sway and roll motion. This prediction to some degree is indicated by the experimental data, and will be examined more closely as the results are discussed.

As a final comment on the mathematical model, it should be said that the two-dimensional model provides loading and motion results which are in very reasonable agreement with experimental results. The two-dimensionalization admittedly introduces errors into the calculation, particularly resulting in frequency shifts of the loading and motion peaks. The error is expected to be larger for the conventional shaped catamarans whose hulls deviate more from a two-dimensional form than do the SWATH ships. The effect of the two-dimensional approximation will be indicated as the loading results are examined.

Results and Discussion

The regular wave results for bending moment and vertical shear based upon the theoretical model just described have been computed and compared to experimental data for two conventional shaped catamarans, ASR and CVA, and one SWATH ship, MODCAT. The geometric information on these models is given in Table 2 and their body plans in Figure 5. By using the transfer functions obtained in regular waves together with the Pierson-Moskowitz sea spectrum, the statistical bending and vertical shear amplitudes have also been computed as a function of significant wave height.

In the following, the discussion on the results will be made for each model:

ASR Catamaran

The results shown in Figure 14 are the predicted and experimental amplitudes of the bending moment, vertical shear force, heave motion, and roll motion for the ASR as a function of the ratio of the wavelength to overall beam (λ/B_m). The amplitude for bending moment has been nondimensionalized by the total ship displacement times the wave amplitude ($\Delta_2 A$), the shear force by the total ship displacement times the wave amplitude divided by the ship length ($\Delta_2 A/L$), the heave motion by wave amplitude (A), and roll motion by the wave slope ($KA = 2\pi A/\lambda$). As mentioned previously, three-dimensional theoretical results were obtained by multiplying the two-dimensional results for the midship section by an equivalent ship length. Experimental results are from ASR model tests performed by Wahab, et al., [4] for a hull separation distance(between the inner hulls) to beam ratio of 1.41.

It is seen that in both shape and magnitude the experimental and theoretical results are in relatively good agreement. It is known that the apparent frequency shift of the moment and shear responses and the sharply peaked nature of the heave and roll responses are due to the two-dimensional approximation.

It is of some interest to examine the separate effects which the incident and diffracted wave and body motion have on the loading quantities. In Figures 17a and 17b the bending moment and vertical shear are plotted showing the various component effects. The broken line curves represent the loading due to the undisturbed incident waves. The dotted curves show the sum of the effects contributed by the undisturbed incident waves and the diffracted waves and represent the restrained body loading. The solid line curves show the addition of motion effects to the restrained body case and are simply a replot of Figures 14a and 14b. It is apparent from Figures 17a and 17b that the magnitude of the bending moment and vertical shear peaks are largely affected by both diffraction and motion effects. It is also clear that all of the components affect both the shape and magnitude of the loading responses to a significant extent and that any attempt to approximate the problem by neglecting either diffraction or motion effects would not appear to be justified.

It was mentioned in the presentation of the theory that if the loading is computed at the middle of the cross-beam structure, heaving should affect only the bending moment and rolling only the vertical shear. This effect is not particularly apparent from the experimental data for conventional shaped catamarans, since the roll and heave resonances are approximately at the same frequency. This point, however, will be

clearly indicated for the example of a SWATH ship where the roll and heave resonances are widely separated in frequency.

CVA Catamaran

The CVA is a conventional catamaran of large beam and shallow draft. Experimental and theoretical values for the loads and motion in regular beam seas are plotted in Figure 15. The resolution of the bending moment and vertical shear into component effects are also shown in Figures 17c and 17d. All quantities have been nondimensionalized in a manner similar to the ASR results. Experimental results were obtained by the second author on a CVA model with the design hull spacing.

Generally good agreement between theoretical and experimental values is indicated. A frequency shift in the peak values of bending moment and vertical shear due to the two dimensionalization is also noted. The important effects of diffraction and motion to the loading calculation is indicated in Figures 17c and 17d.

MODCAT

An example of the loading and motion of a SWATH ship was obtained for the MODCAT model 5266. The loading and motion responses in regular beam waves are shown in Figure 16. Resolution of the bending moment component effects is also shown in Figure 18. All nondimensionalizations are accomplished in the manner described previously.

Excellent agreement between theoretical and experimental results for the bending moment is shown in Figure 16a. Figure 18 shows that the large peak in the bending moment is almost totally a result of wave diffraction effects. Both experimental and theoretical data indicate the very large roll resonance at long wavelengths as shown in Figure 16d, however, this roll resonance does not appear to be reflected at all in

the bending moment. This confirms the contention made earlier that the roll should not affect the bending moment at the midpoint of the cross-beam. Figure 18 shows the relatively small influence that heaving motion has on the bending moment.

Very poor agreement in the vertical shear for the MODCAT shape is shown in Figure 16b. This poor agreement is almost cretainly due to the difficulty which has been encountered in theoretically predicting the damping coefficient for the SWATH shpaes and to a lesser extent for conventional catamaran forms. In the present mathematical models for motion the damping is modified on the basis of the experimental results of motion. Such a modification in the roll damping was made to obtaine the good agreement shown for roll motion in Figure 16d; however, an analogous modification for the loading is not as straightforward and consequently has not yet been applied to the vertical shear computation. This defect is considered to be the main cause for the poor agreement.

As a final comment on the regular-wave loading results, it is interesting to compare the bending moments for the three catamarans. The CVA shows a nondimensional peak bending moment significantly smaller than the other two ships. Because the CVA is a shallow draft ship, this shows that a large part of the bending moment is contributed by the horizontal pressure force acting with a given vertical moment arm. This suggests that an important criterion for minimizing the bending moment of the cross-beam, would be to reduce the draft and/or reduce the height of the cross-beam above the waterline.

Loading in Irregular Beam Seas

Under similar assumptions made in the prediction of motion in irregular seas [5] the statistical amplitudes for bending moment and vertical shear are given as follows:

$$E = \int_0^\infty [R(\omega_i)]^2 \, S(\omega_i) \, d\omega.$$

where $R(\omega)$ is the amplitude response of bending moment or shear force to a wave of unit amplitude and frequency, ω_e. In nondimensional form $R(\omega_i)$ is simply the regular wave loading responses obtained previously. $S(\omega_i)$ is the Pierson-Moskowitz Sea strectrum as defined by Equation (4).

Statistical amplitudes of loading are then defined as:

Significant	$C_{1/3}$	$= 2 \; E$
Average	$C_{1/2}$	$= 1.253 \; E$
One-Tenth Highest	$C_{1/10}$	$= 2.546 \; E$

The significant amplitude of the bending moment and vertical shear force is plotted as a function of significant wave height for the ASR, CVA, and MODCAT in Figure 19.

Bending moment has been nondimensionalized with respect to the displacement of one hull times the distance from the catamaran centerline to the centerline of one hull ($\Delta_1 b$) and the shear has been nondimensionalized with respect to the displacement of one hull (Δ_1).

SUMMARY

1. Correlation of analytical predictions of heave and pitch motion in head seas and hydrodynamic loads on the cross deck in beam seas have been made.

2. The analytical prediction of the motion is satisfactory except near the resonant encountering frequencies. Here, the magnitude of the motion amplitudes is overestimated and increases with the forward speed. The pehnomenon is particularly so for SWATH configurations. The analytical prediction of the hydrodynamic loads on the cross deck induced by beam waves is found satisfactory, despite the two-dimensional analysis adopted in this work, except for the vertical shear of SWATH configuration.

3. The discrepancies observed in the correlation are considered to be caused by an inadequacy of the theory in accounting for viscous effects and three-dimensional hydrodynamic interaction effects between the two hulls especially for high speeds.

4. Two distinct dimensions associated with catamarans are the separation distance between the two demihulls and the cross-deck height above the waterline. Except for roll motion, the effect of the separation distance on motion and wave-induced loads seems not so significant when the separation distance between the inner hulls is within 70 to 140 percent of the demihull beam. The cross-deck height has direct effect on the cross-deck slamming and the bending moment on the cross-deck. It appears from the present analysis that an increase in the deck height increases the bending moment but obviously decreases the chance of the slamming.

5. From the hydrodynamic load analysis, it is obvious that the analysis based on the static pressure over the hull surface or on the so called Froude-Krylov approach is inadequate to provide accurate results. This means that the effect of the wave diffraction by the body and the effect of motion should be taken into account in the analysis.

ACKNOWLEDGEMENT

The authors would like to acknowledge the contributions made to the work presented in this paper by many NSRDC personnel who have been engaged in the exploratory development of naval catamarans. Particularly, the authors would like to express their thanks for Mr. Hadler's critical review of the paper and valuable suggestions.

The authors also would like to acknowledge the funding supports provided by the NSRDC In-House Independent Research Program, the General Hydromechanics Research Program, the SWATH Ship Program and the Research, Development, Test and Evaluation Program of NAVSHIPS.

REFERENCES

1. Salvesen, N, Tuck, E.O. and Faltinsen, O., "Ship Motions and Sea Loads," SNAME Trans. Vol. 78 (1970), pp. 250-287.

2. Jones, H.D., "Catamaran Motion Predictions in Regular Waves," NSRDC Report 3700 (1972) pp. 27.

3. Pien, P.C. and Lee, C.M., "Motion and Resistance of a Low-Waterplane-Area Catamaran," presented at the 9th Symposium on Naval Hydromechanics in Paris (1972).

4. Wahab, R., Pritchett, C., and Ruth, L.C., "On the Behavior of the ASR Catamaran in Waves," Marine Technology, Vol. 8, No. 3, (1971).

5. St. Denis, M. and Pierson, W.J., "On the Motion of Ships in Confused Seas," SNAME Trans., Vol. 61 (1953) pp. .

6. Pierson, W.J. and Moskowitz, L., "A Proposed Spectral Form for Fully Developed Wind Seas, Based on the Similarity Theory of S.A. Kitaigarodsku," Journal of Geophysical Research, Vol. 69, No. 24 (1964) pp. 5181-5190.

7. Ochi, M.D. and Bonilla-Norat, J., "Pressure-Velocity Relationship in Impact of the Ship Model Dropped onto the Water Surface and in Slamming in Waves," NSRDC Report 3153 (1970).

8. Ochi, M.K., "Prediction of Occurrence and Severity of Ship Slamming at Sea," The 5th Symposium on Naval Hydromechanics (1964) pp. 545-595.

9. Lee, C.M., Jones, J. and Bedel, J.W., "Added Mass and Damping Coefficients of Heaving Twin Cylinders in a Free Surface," NSRDC Report 3695 (1971).

10. Jones, H.D. and Gerzina, D.A., "Motion and Hull Induced Bridging Structure Load Characteristics for a Large Modified CVA Catamaran in Waves," NSRDC Report 3819 (in review).

11. Ogilvie, T.F., "On the Computation of Wave-Induced Bending and Torsion Moment," Journal of Ship Research, Vol. 15, No. 3 (1971), pp. 217-220.

FIGURES AND TABLES

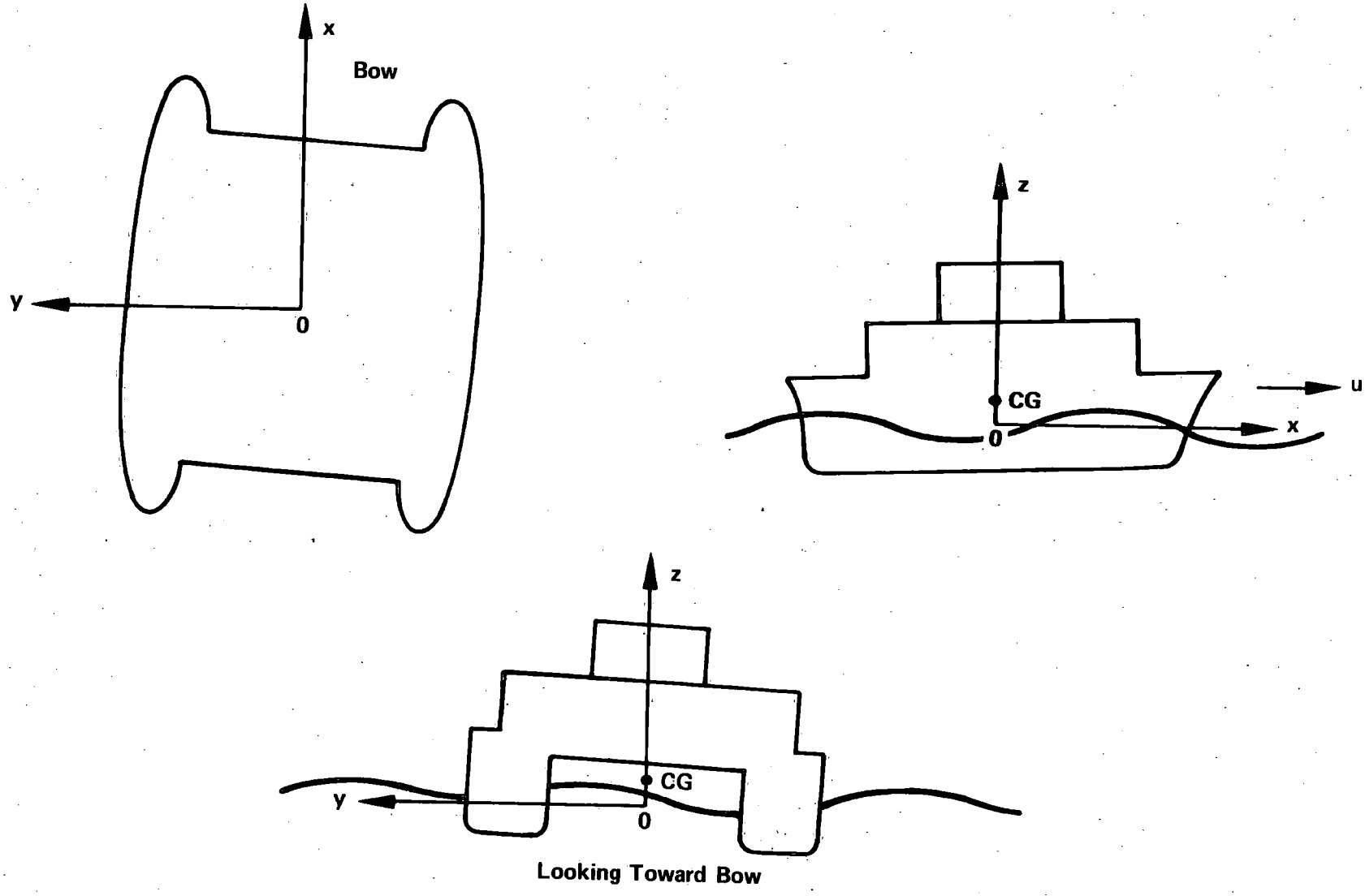

Figure 1 — Coordinate system

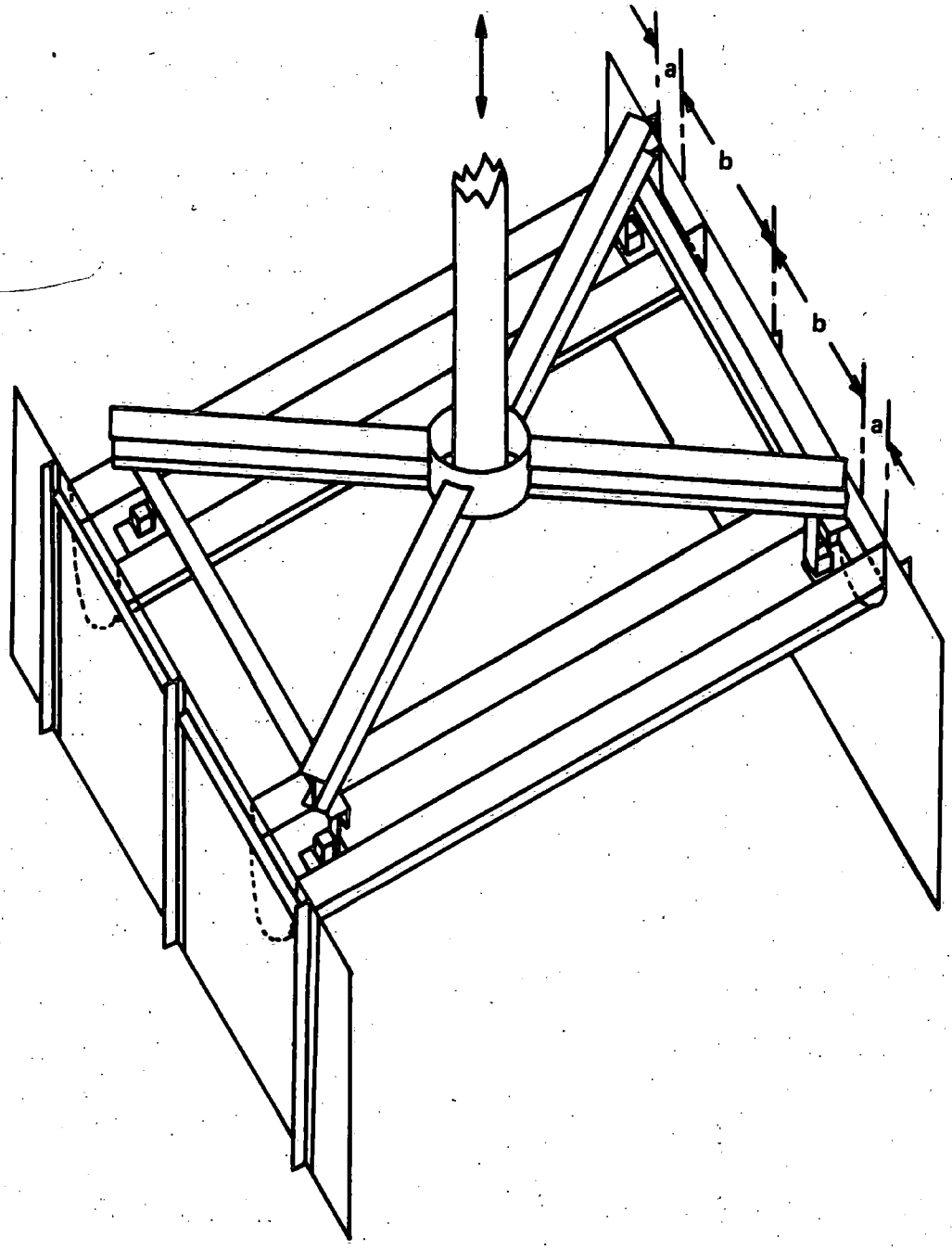

Figure 2 – Two-dimensional model setup for testing

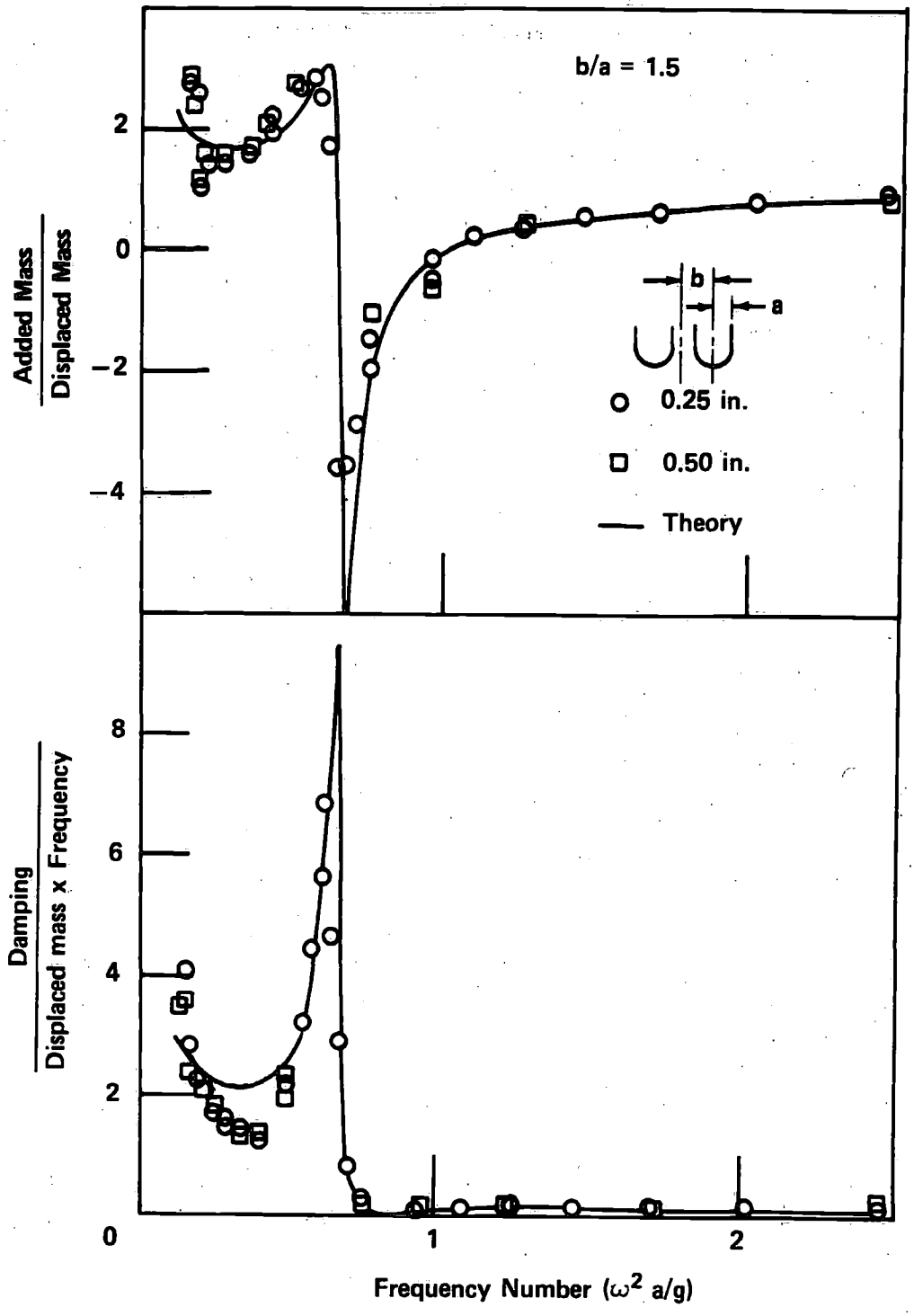

Figure 3 — Added mass and damping coefficients versus frequency number for twin semicircular cylinders for b/a = 1.5

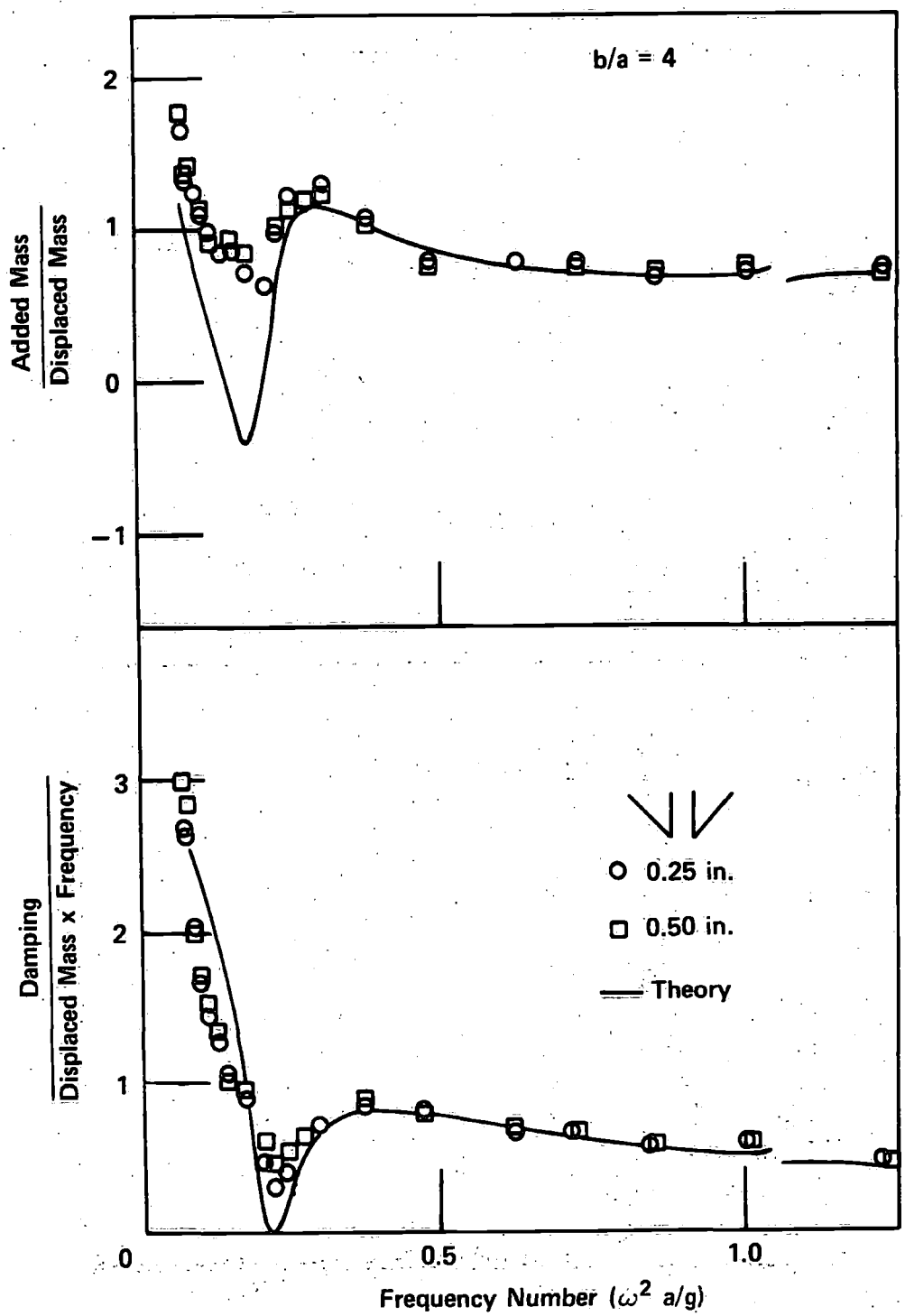

Figure 4 — Added mass and damping coefficients versus frequency number for twin right triangles for b/a = 4

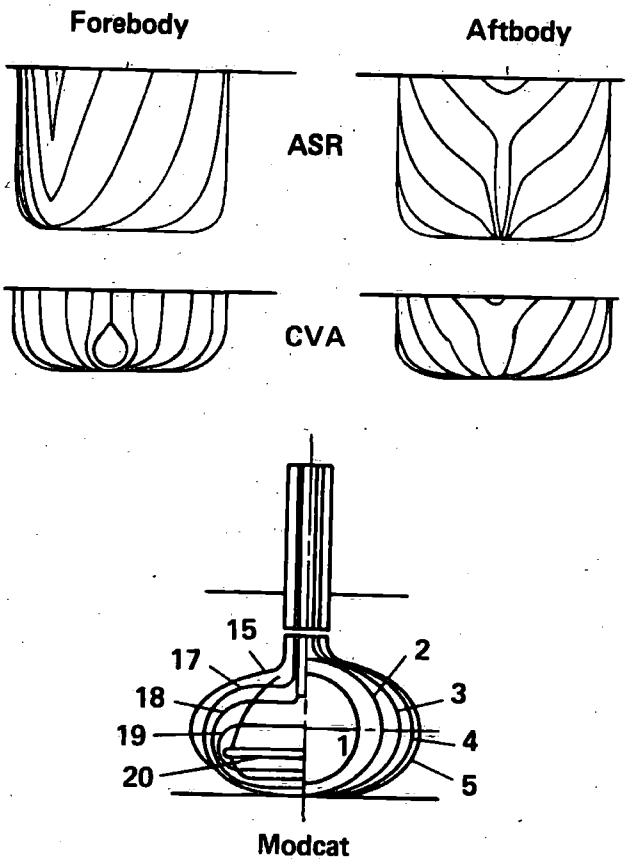

Figure 5 – Body plans

Table 1 — Particular dimensions

Particular	ASR	CVA	MODCAT
NSRDC Model Number	5061	5,228	5,266
Beam (Each Hull) in Feet at the Waterline	24.0	95.8	30.42
Draft in Feet (Station 10)	18.0	36.5	69.5
Length in Feet at the Waterline	210.0	820.0	850.0
Displacement of Each Hull in Long Tons	1386 (S.W.)	47,400 (S.W.)	50,500 (S.W.)
Hull Spacing in Feet	38.0	141.2	207.0
Longitudinal Center of Gravity Aft of F. P. in Feet	105.6	419.0	420.0
Longitudinal Radius of Gyration in Feet	0.233L	0.23L	0.26L
Block Coefficient	0.55	0.59	0.964
Scale Ratio	16.89	54.67	50.0
Diameter in Feet	—	—	—
Vertical Height of Neutral Axis from Mean Waterline in Feet	23.0	61.5	68.2

TABLE 2

Comparison of restoring coefficients for ASR

Coefficient	Experimental	Computed
C_{33}	14.3	15.6
C_{53}	0.499	0.508
C_{35}	0.511	0.508
C_{55}	0.739	0.853

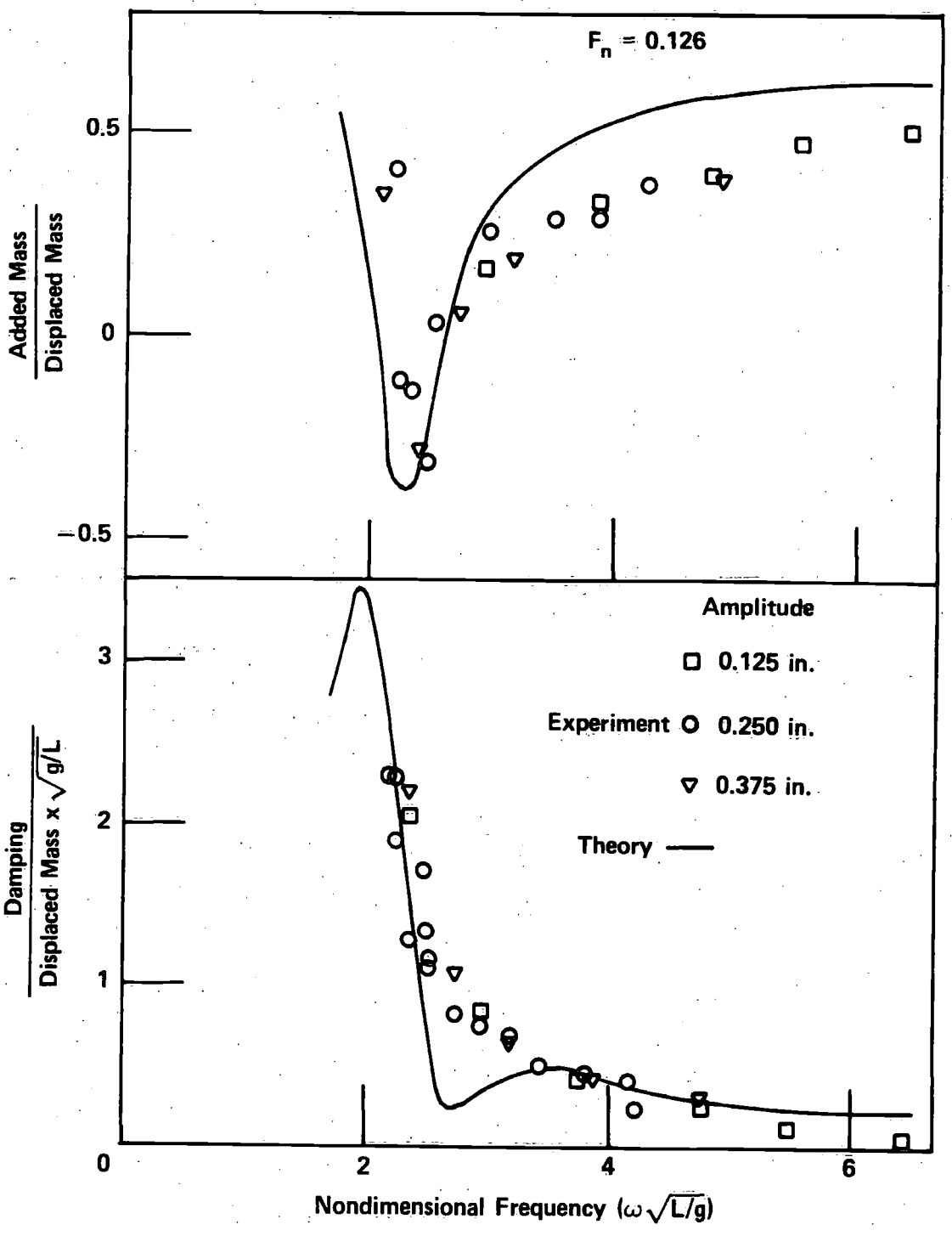

Figure 6 — Heave added mass and damping coefficients versus nondimensional frequency for the ASR

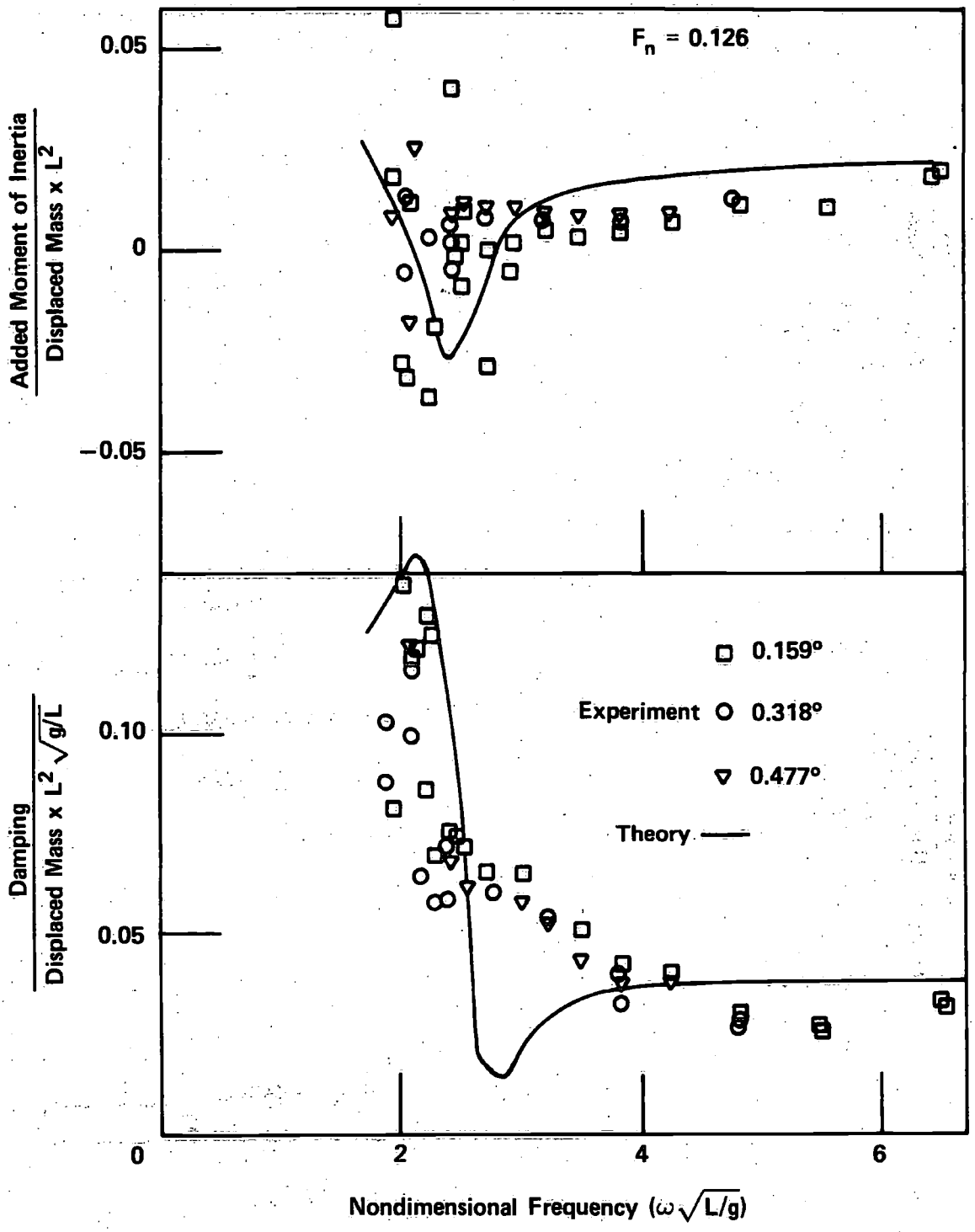

Figure 7 — Pitch added moment of inertia and damping coefficients versus nondimensional frequency for the ASR

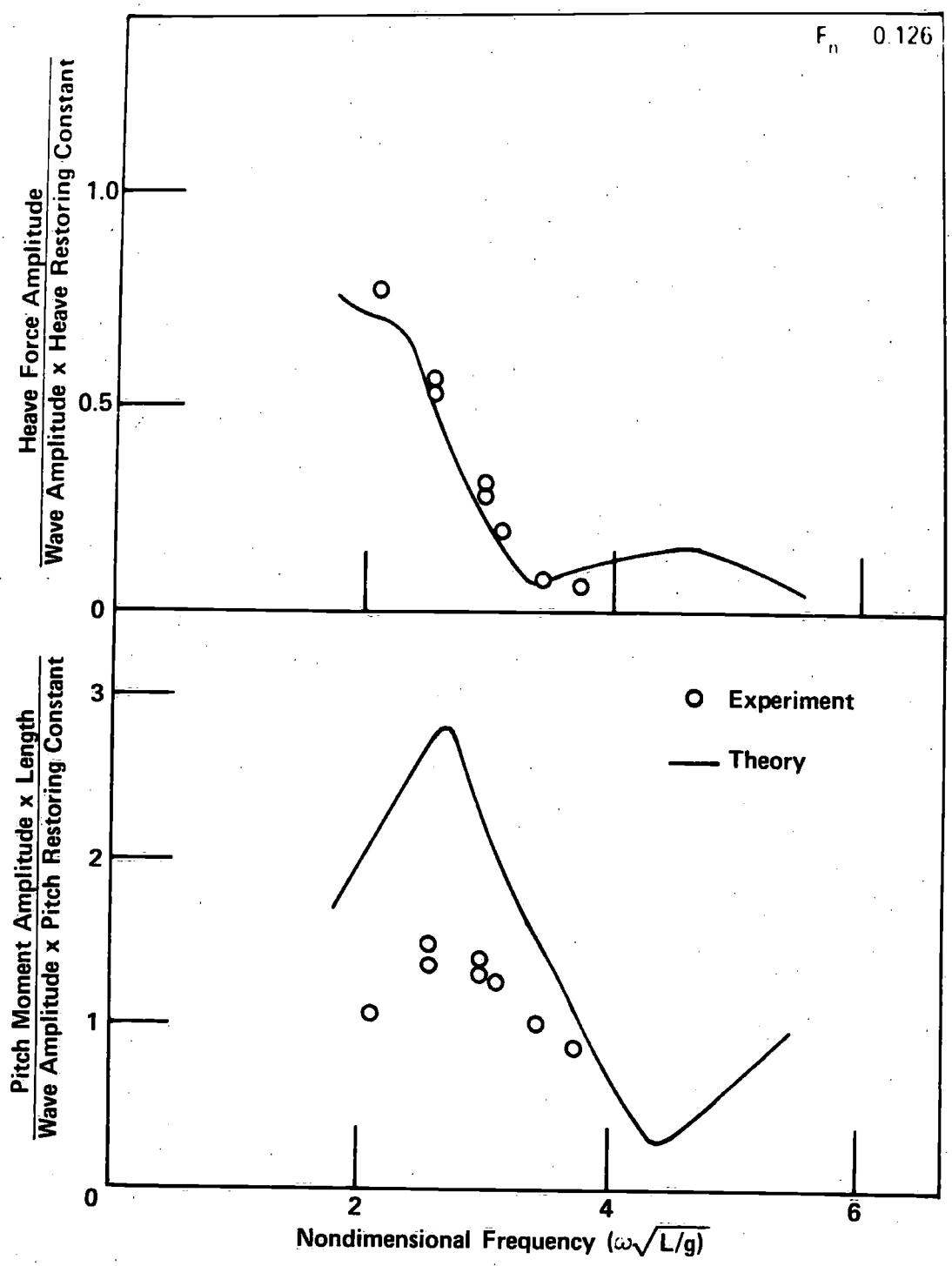

Figure 8 – Heave exciting force and pitch exciting moment parameters versus nondimensional frequency for the ASR

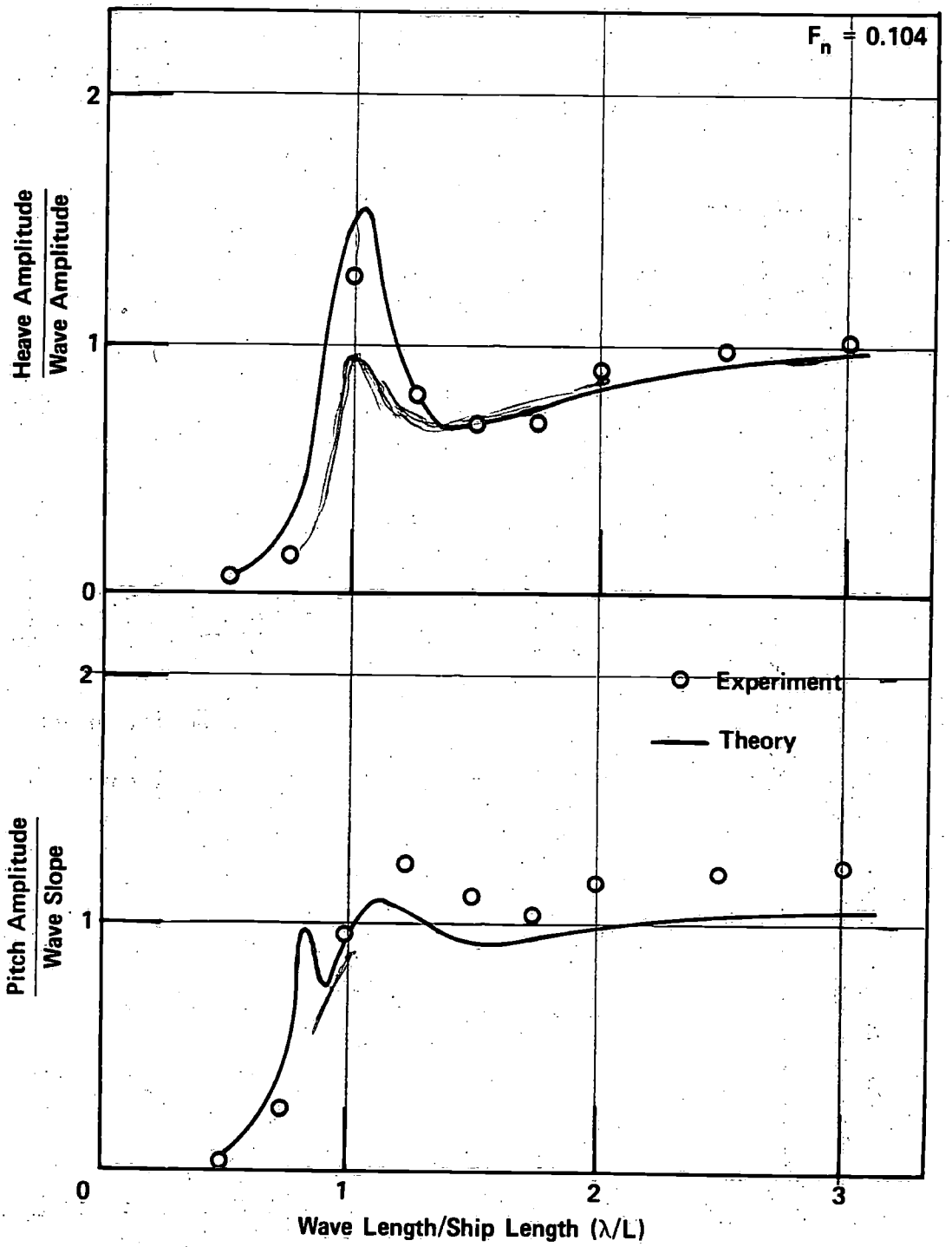

Figure 9 — Nondimensional heave and pitch amplitudes versus wave length to ship length ratio for the ASR

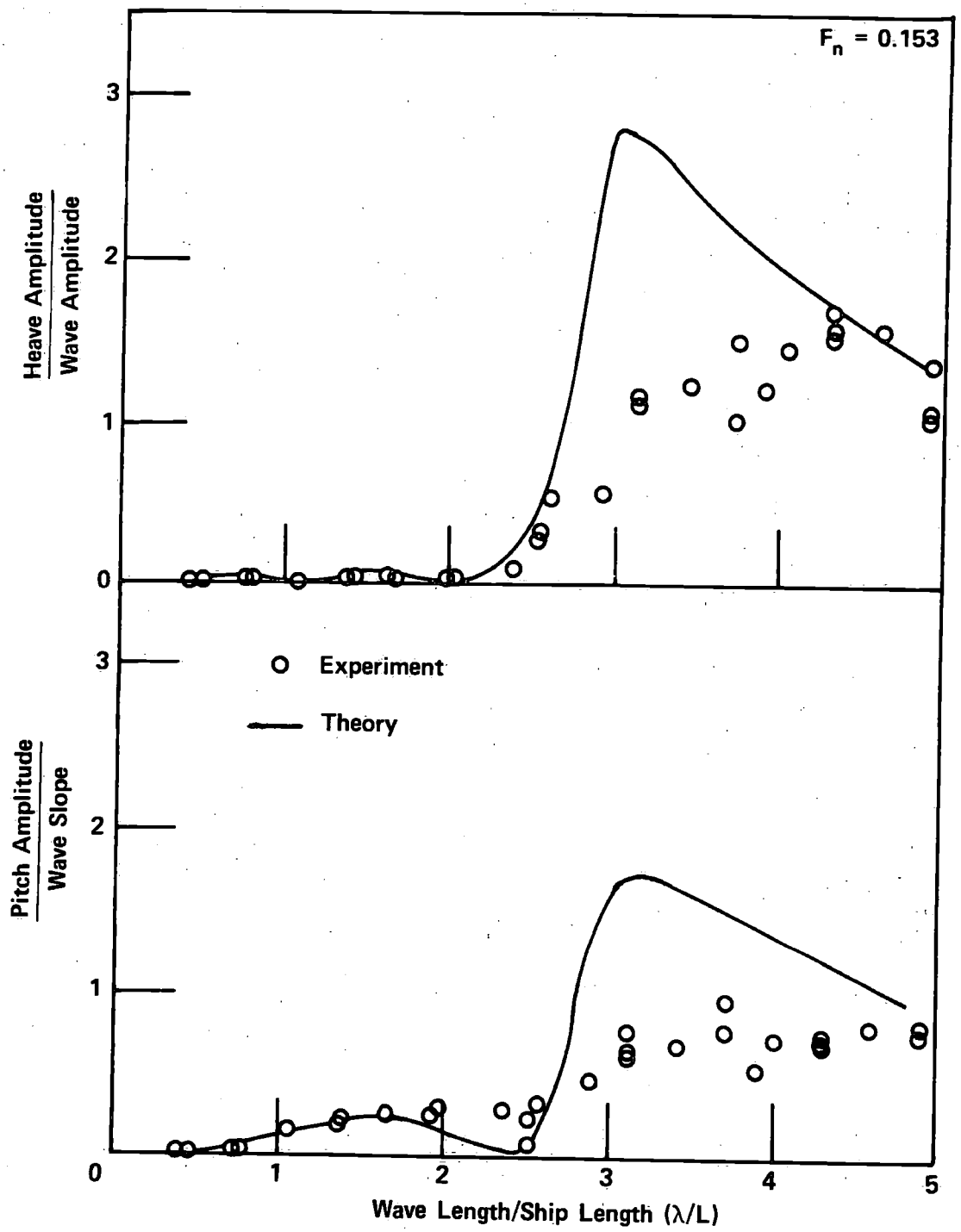

Figure 10 — Nondimensional heave and pitch amplitudes versus wave length to ship length ratio for the MODCAT

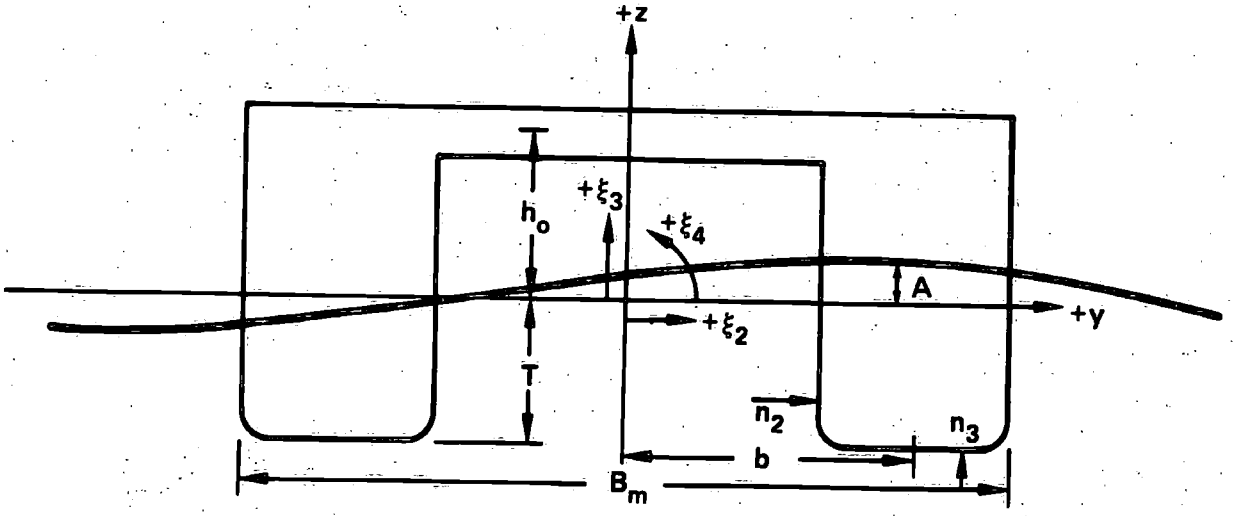

Figure 11 — Geometry and conventions

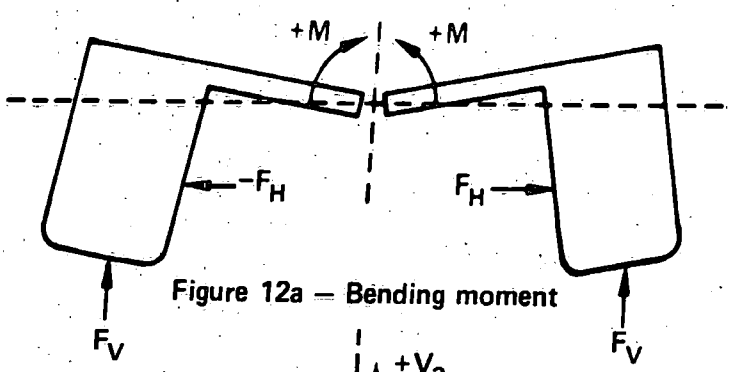

Figure 12a — Bending moment

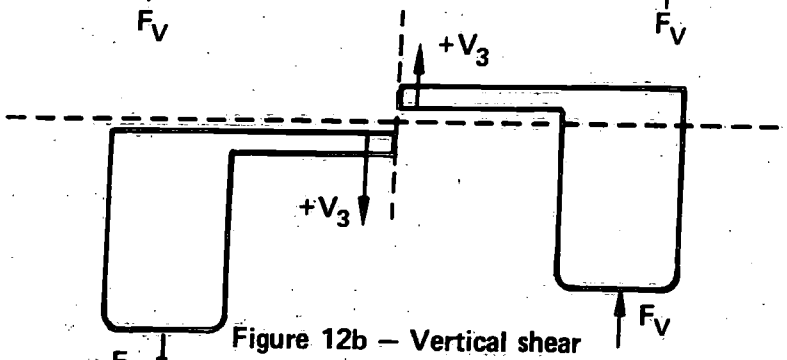

Figure 12b — Vertical shear

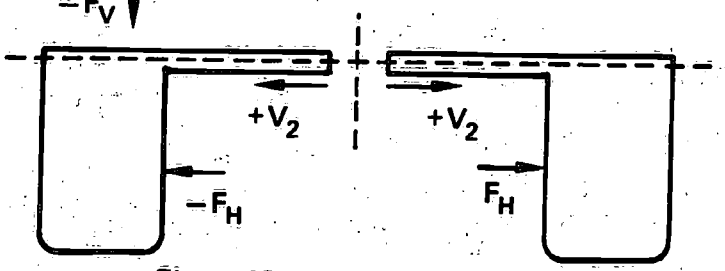

Figure 12c — Horizontal shear

Figure 12 — Loading conventions

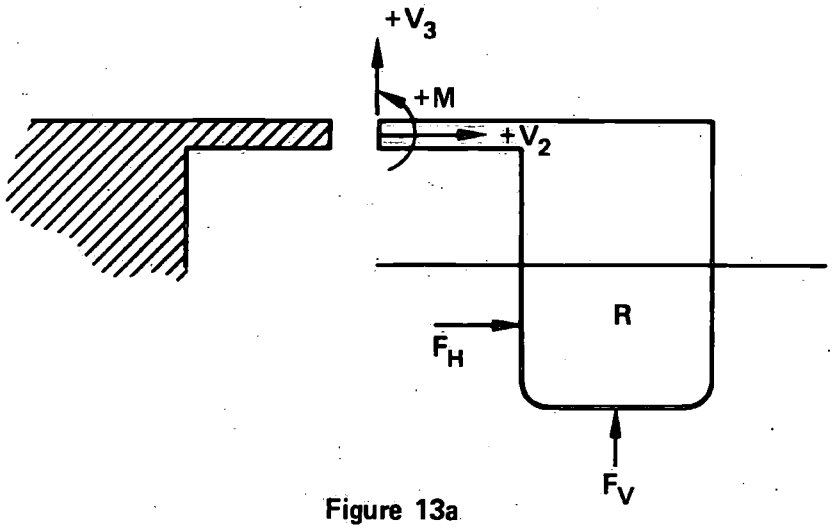

Figure 13a

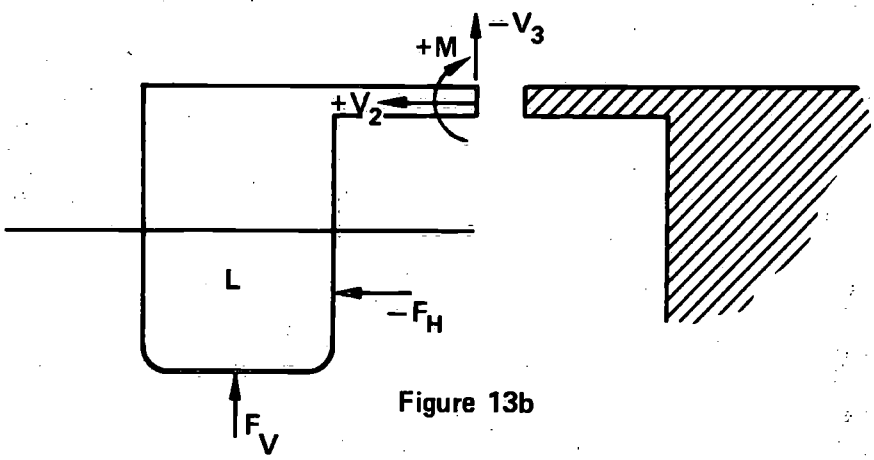

Figure 13b

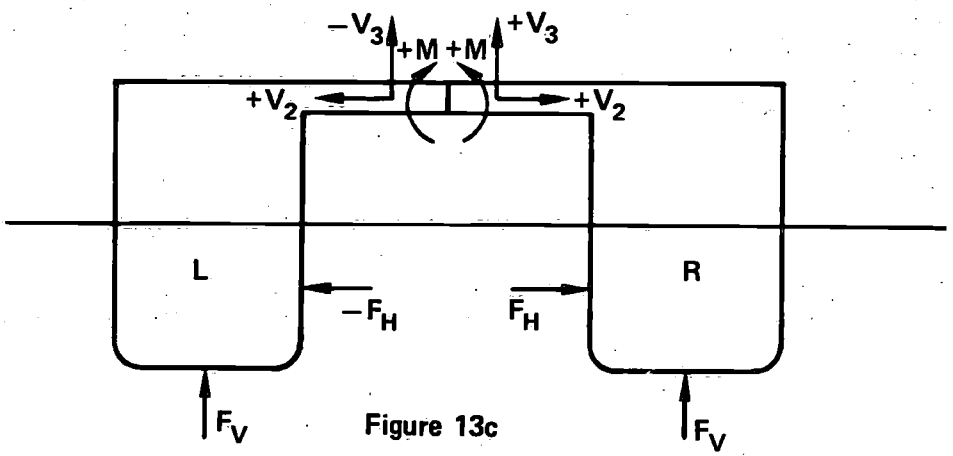

Figure 13c

Figure 13 — Loading analysis diagram

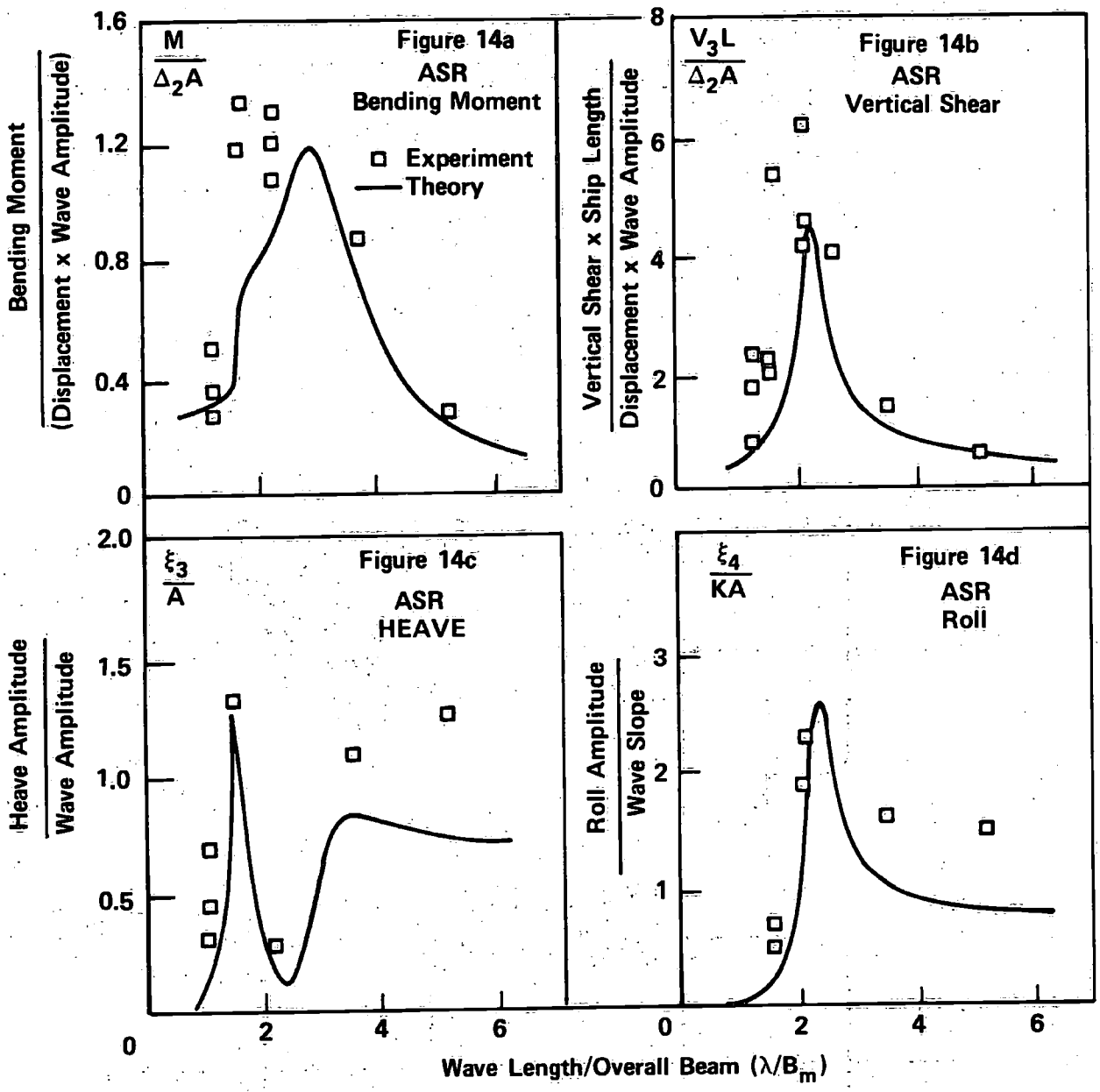

Figure 14 – Loading and motion of ASR in regular beam waves for zero speed

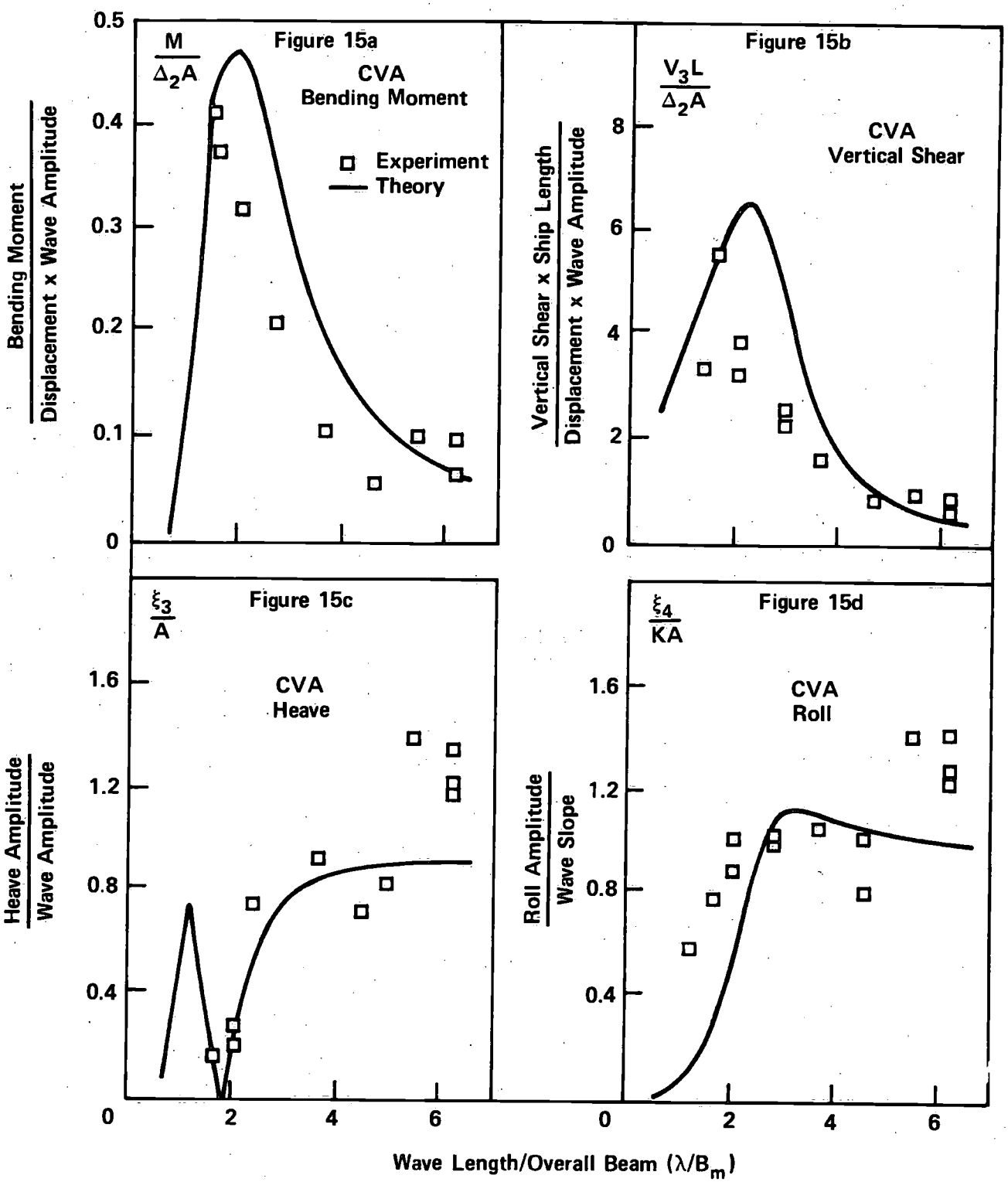

Figure 15 — Loading and motion of CVA in regular beam waves for zero speed

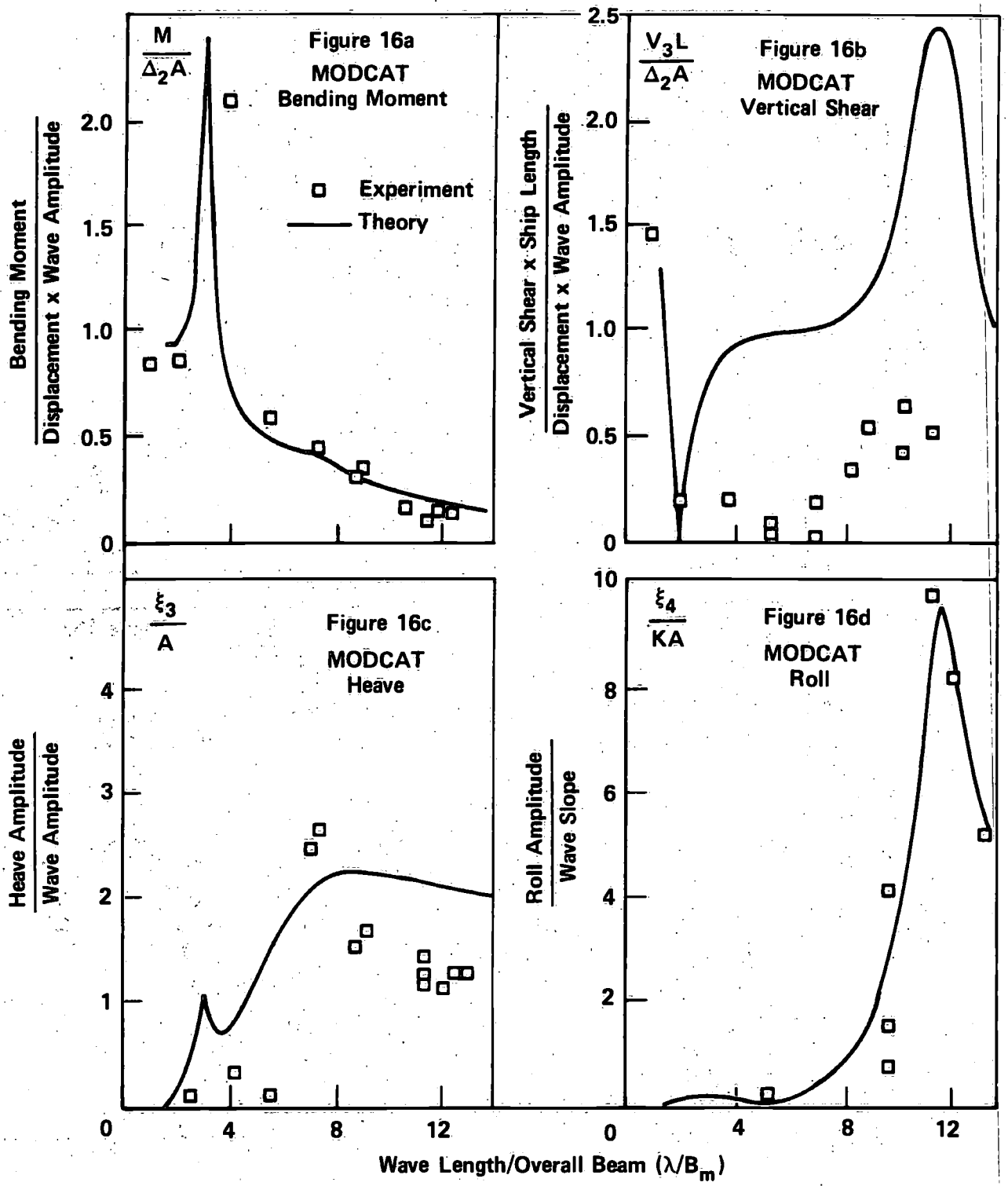

Figure 16 — Loading and motion of MODCAT in regular beam waves for zero speed

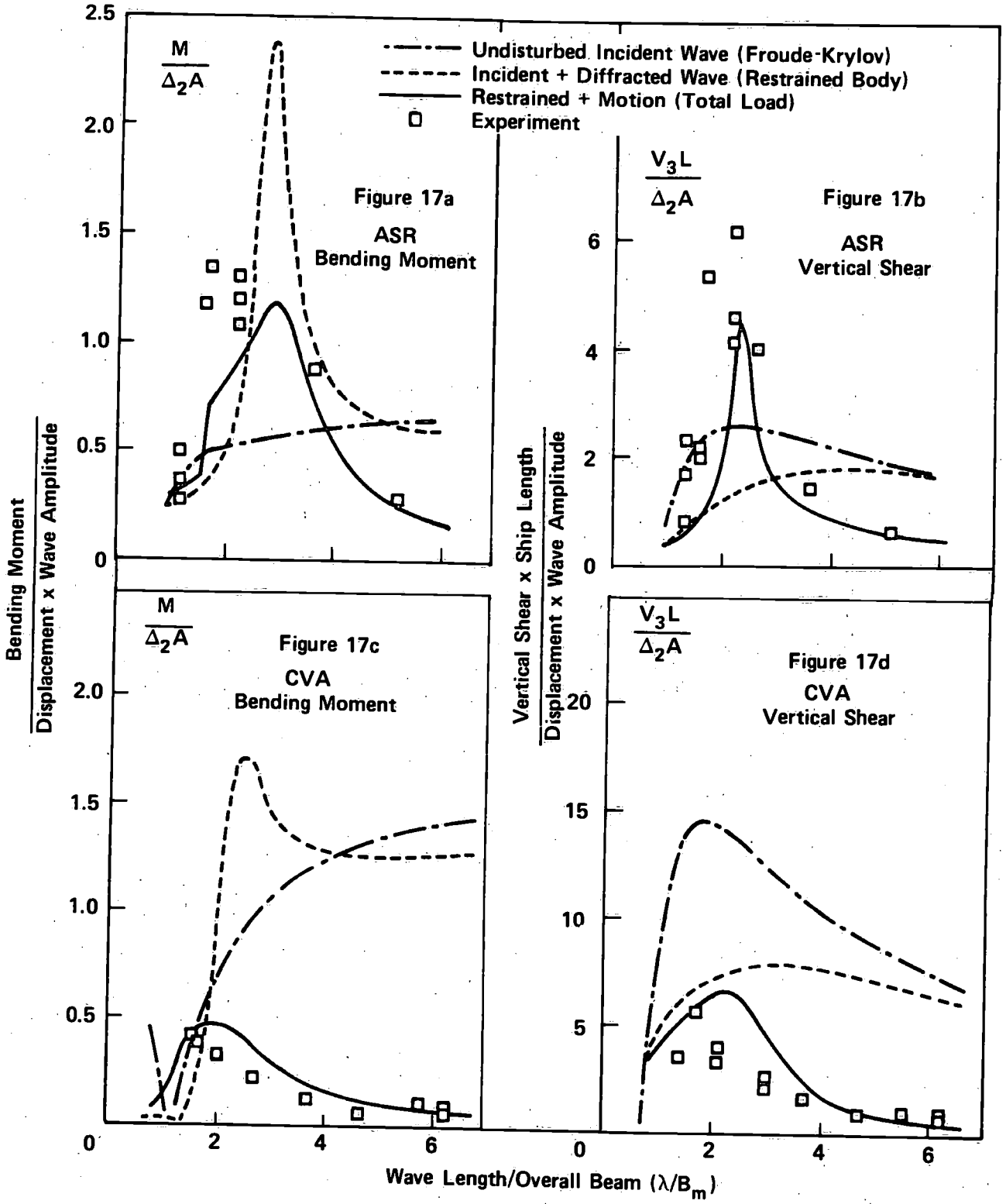

Figure 17 — Decomposition of loading effects for ASR and CVA

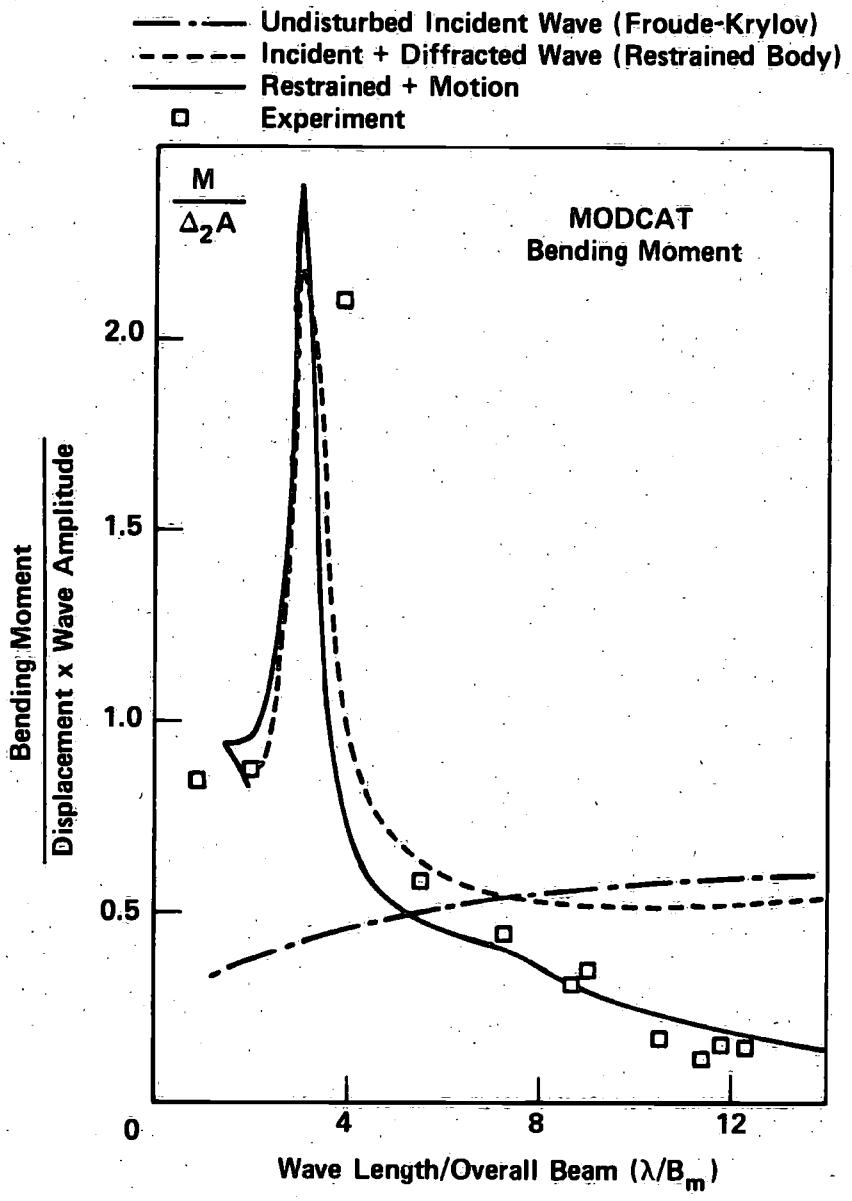

Figure 18 — Decomposition of bending moment effects for MODCAT

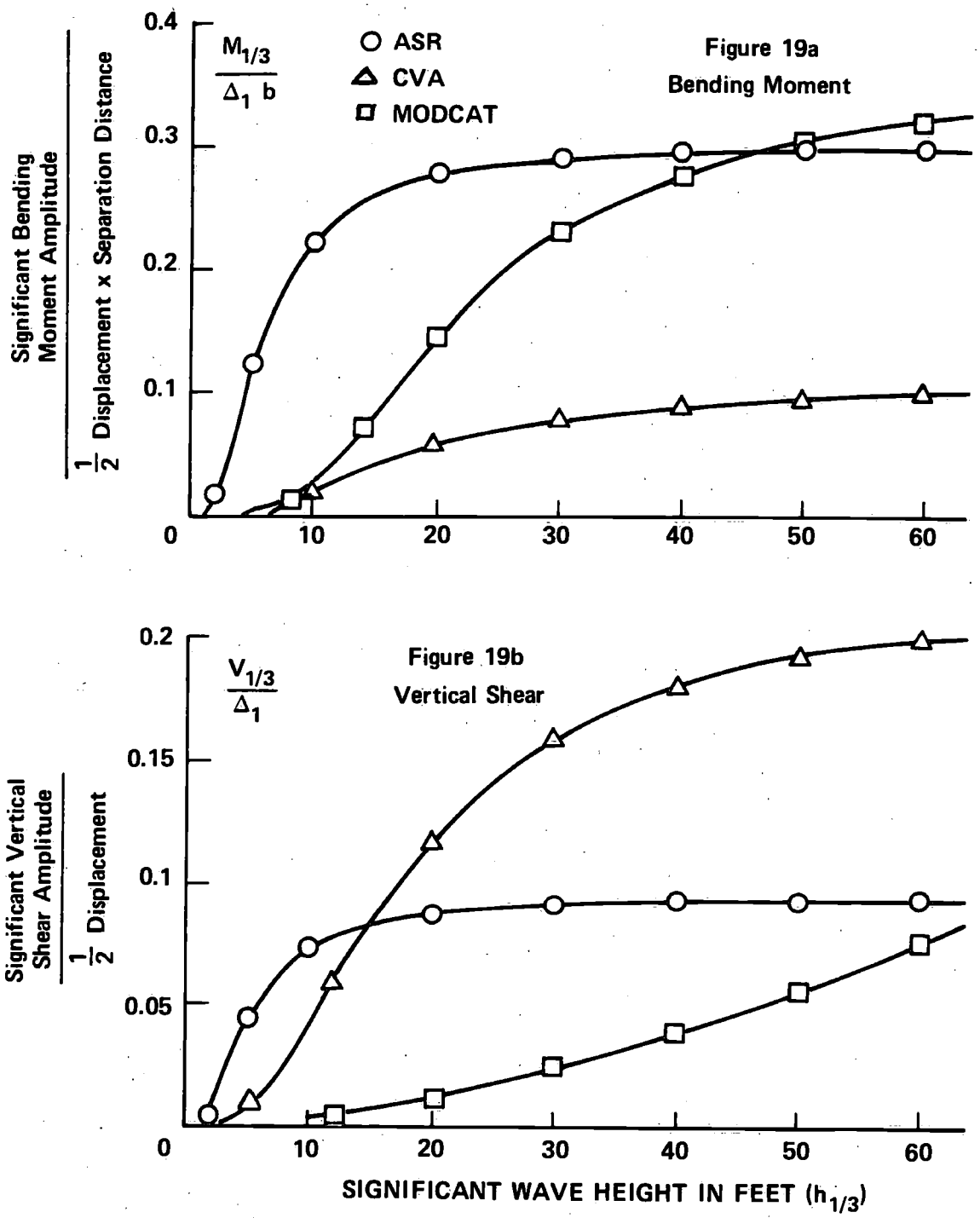

Figure 19 — Catamaran loading in irregular beam seas